nature aging

Letter

https://doi.org/10.1038/s43587-024-00744-7

Late-life protein or isoleucine restriction impacts physiological and molecular signatures of aging

Received: 9 January 2024

Accepted: 10 October 2024

Published online: 27 November 2024

Check for updates

Chung-Yang Yeh[1,2], Lucas C. S. Chini[1,2], Jessica W. Davidson[3], Gonzalo G. Garcia[4], Meredith S. Gallagher[1,2], Isaac T. Freichels[1,2], Mariah F. Calubag[1,2,5], Allison C. Rodgers[1,6], Cara L. Green[1,2], Reji Babygirija[1,2,5], Michelle M. Sonsalla[1,2,7], Heidi H. Pak[1,2,8], Michaela E. Trautman[1,2,8], Timothy A. Hacker[1,6], Richard A. Miller[4], Judith A. Simcox[3,9] & Dudley W. Lamming[1,2,5,7,8,10,11]

Restricting the intake of protein or the branched-chain amino acid isoleucine promotes healthspan and extends lifespan in young or adult mice. However, their effects when initiated in aged animals are unknown. Here we investigate the consequences of consuming a diet with 67% reduction of all amino acids (low AA) or of isoleucine alone (low Ile), in male and female C57BL/6J.Nia mice starting at 20 months of age. Both dietary regimens effectively promote overall metabolic health without reducing calorie intake. Both low AA and low Ile diets improve aspects of frailty and slow multiple molecular indicators of aging rate; however, the low Ile diet reduces grip strength in both sexes and has mixed, sexually dimorphic effects on the heart. These results demonstrate that low AA and low Ile diets can promote aspects of healthy aging in aged mice and suggest that similar interventions might promote healthy aging in older adults.

In defiance of the paradigm that energy intake alone determines the resulting physiology, there is a growing recognition that calories sourced from different macronutrients are not equivalent[1]. In particular, dietary protein is emerging as a dominant regulator of metabolism and healthy aging. Several retrospective and prospective clinical trials have found that diets with lower levels of protein are associated with decreased rates of age-related diseases, as well as with an overall reduction of mortality in those under age 55 years[2,3]. While the effect of long-term protein restriction (PR) on human aging has not been tested in a randomized clinical trial, short-term randomized clinical trials in people who are overweight or have diabetes have found that PR promotes metabolic health, reducing adiposity and improving glycemic control, even when the calories consumed by the PR group were not limited[4,5]. PR has also been repeatedly shown to increase the health and lifespan of model organisms, including flies and rodents[6–10].

PR necessarily restricts dietary essential amino acids (AAs), including the three branched-chain AAs (BCAAs; leucine, isoleucine and valine). We and others have shown that restricting the three BCAAs benefits metabolic health in mice and rats, improving glucose tolerance and reducing adiposity[10–13]. The restriction of BCAAs extends lifespan and reduces frailty in male mice, while dietary supplementation with additional BCAAs shortens lifespan in both sexes[10,14]. We have shown

[1]Department of Medicine, University of Wisconsin–Madison, Madison, WI, USA. [2]William S. Middleton Memorial Veterans Hospital, Madison, WI, USA. [3]Department of Biochemistry, University of Wisconsin–Madison, Madison, WI, USA. [4]Department of Pathology, University of Michigan School of Medicine, Ann Arbor, MI, USA. [5]Graduate Program in Cellular and Molecular Biology, University of Wisconsin–Madison, Madison, WI, USA. [6]Cardiovascular Physiology Core Facility, University of Wisconsin–Madison, Madison, WI, USA. [7]Comparative Biomedical Sciences Graduate Training Program, University of Wisconsin–Madison, Madison, WI, USA. [8]Nutrition and Metabolism Graduate Program, University of Wisconsin–Madison, Madison, WI, USA. [9]Howard Hughes Medical Institute, Department of Biochemistry, University of Wisconsin–Madison, Madison, WI, USA. [10]University of Wisconsin–Madison Comprehensive Diabetes Center, Madison, WI, USA. [11]University of Wisconsin Carbone Cancer Center, Madison, WI, USA. e-mail: dlamming@medicine.wisc.edu

that reductions in the BCAA isoleucine alone is both necessary and sufficient for many of the metabolic benefits of PR in young male mice[13]. In humans, dietary isoleucine levels, but not levels of leucine or valine, are strongly correlated with body mass index[13]. Finally, restriction of isoleucine in adult mice extends lifespan in both males and females[15], and in humans, blood levels of isoleucine, but not of leucine or valine, are positively associated with mortality[16]. Thus, there is substantial evidence that dietary isoleucine is a critical regulator of metabolic health and aging in both mice and humans.

Almost all previous studies of isoleucine or PR have been conducted on young adult mice, but many geroprotective interventions, such as calorie restriction, have blunted benefits when starting in mid-life or later[17]. This represents a critical knowledge gap. To better understand the effects of restricting protein or isoleucine late in life, we placed 20-month-old C57BL/6J.Nia mice of both sexes on diets in which either all AAs (low AA) or isoleucine alone (low Ile) was restricted by 67%. At this age, C57BL/6J mice are estimated to be roughly equivalent to 60-year-old humans[18]. We examined the physiology, fitness and frailty of these mice longitudinally over 4 months, finding that both low AA and low Ile diets improved overall metabolic health and favorably impacted molecular aging rate indicators. Finally, we found that a low Ile diet favorably remodels the aging heart in females and reverses many age-associated changes in hepatic gene expression in both sexes. Our findings suggest that restricting dietary protein or isoleucine may promote aspects of healthy aging even when initiated later in life.

Results

Low AA and low Ile diets reduce weight and adiposity in aged mice

To examine the effects of PR and isoleucine restriction as late-life interventions, we fed 20-month-old male and female C57BL/6J.Nia mice from the National Institute on Aging (NIA) aged mouse colony one of three AA-defined diets. These diets include the control diet (control; TD.140711), with 22% of its calories derived from protein, a diet in which isoleucine was reduced by 67% (low Ile; TD.160734) and a diet in which all 20 AAs were reduced by 67% (low AA; TD.140712). We placed an additional group of 6-month-old mice on the control diet as the young control group (young control). All three diets are isocaloric, with identical levels of fat. In the low Ile diet, nonessential AAs were increased to keep the calories derived from AAs constant, while in the low AA diet, carbohydrate levels were increased. All three of these diets have been used previously (Extended Data Table 1)[13,15].

We characterized the effects of these diets on the aged mice over 4 months (Fig. 1a). In males, the aged control-fed mice maintained their weight throughout the course of the experiments, while the aged low Ile-fed mice lost weight rapidly and the aged low AA-fed mice lost weight more gradually (Fig. 1b,c). Aged low Ile-fed males had decreased fat and lean mass, whereas the weight loss of aged low AA-fed males was due to the loss of lean mass (Fig. 1c and Extended Data Fig. 1a,b). Both low Ile and low AA-fed males had an overall decrease in adiposity at every time point examined (Fig. 1d). Similar effects of low Ile and low AA diets on weight and body composition were observed in aged female mice (Fig. 1h–j and Extended Data Fig. 1g,h). Of note, these changes in weight and body composition were not due to decreased food consumption (Extended Data Fig. 1c,l and Supplementary Fig. 1a,b).

We further examined the effect of these dietary interventions on systemic metabolism. In alignment with our previous observations in young mice, both low Ile and low AA feeding induced the energy balance hormone FGF21 (Fig. 1e,k). Similarly, both low Ile and low AA feeding improved glucose tolerance, with the low Ile diet also lowering fasting blood glucose (Fig. 1f,l and Extended Data Fig. 1d,j). Neither diet altered insulin tolerance (Extended Data Fig. 1e,k). In a separate cohort of 25-month-old animals, the low Ile diet likewise improved glucose tolerance in both sexes, and the low AA diet improved glucose tolerance in females (Extended Data Fig. 1f,l). Using metabolic chambers to measure respiratory gases and calculate energy expenditure via indirect calorimetry, we found that energy expenditure was elevated in aged low Ile- and low AA-fed mice (Fig. 1g,m). When lean mass was analyzed as a covariate, aged low Ile-fed males, but not females, have reduced energy expenditure (Extended Data Fig. 2a,b). Spontaneous movement did not contribute to these changes in energy balance (Extended Data Fig. 2c,d). Assessing fuel source utilization, we found an increased respiratory exchange ratio in aged low Ile- and low AA-fed mice of both sexes (Extended Data Fig. 2e,f).

Low Ile and low AA diets improve aspects of late-life healthspan

We utilized a validated mouse frailty index to quantify frailty through the accumulation of deficits[19]. Initially, we performed a three-way mixed-effects analysis (REML) to identify the contribution of age, diet and sex. As sex was found to be a contributing factor in the response of low Ile-fed mice (Supplementary Fig. 2a–c), we analyzed the data in a pairwise two-way mixed-effects analysis (REML) with the sexes separated. As expected, frailty increased with age and time (Fig. 2a,h). Despite a modest decrease in frailty in low Ile- and Low AA-fed mice in both sexes, the effects of the diets did not reach statistical significance in either sex (for example, male aged low Ile versus aged control, $P = 0.071$). The categorical parameters and the individual measures that contributed the most to these group scores were analyzed, revealing that the low Ile and the low AA diets robustly reduced deficits in body condition and distended abdomen scores in males (Fig. 2b,c,i,j and Supplementary Fig. 2d–o).

We assessed fitness with an accelerating rotarod and inverted cling tests. As expected, young control-fed mice had the best performance (Fig. 2d,e,k–l). In the rotarod test, aged low Ile-fed males performed significantly better than aged control-fed males, and the performance of both aged low Ile-fed and aged low AA-fed males was comparable to the young control-fed males (Fig. 2d). In contrast, there was no effect of diet on the rotarod performance of aged females (Fig. 2k). In an inverted cling test, we observed a small decrease in the hang time of aged low Ile-fed males and females (Fig. 2e,l). Analyzing these data with body weight as a covariate, we found that, independent of body weight, aged low Ile-fed females performed significantly worse than aged control-fed females on the inverted cling test (Supplementary Fig. 3a–d).

We examined the impact of low Ile and low AA diets on cognition by conducting a novel object recognition test (NOR) and a Barnes maze test (BMT) at approximately 23 months of age. Interestingly, aged control-fed females exhibited increased locomotion during the habituation phase of the NOR compared with both aged low Ile-fed females and the young control-fed females. This effect of diet and age was not observed in males (Supplementary Fig. 4a,b). In the NOR test, we did not observe a significant effect of age or diet during the acquisition phase, the short-term memory test or the long-term memory test in either sex (Supplementary Fig. 4c–e,g–i). The total time investigating both objects was significantly higher in young control-fed males and significantly lower in aged low Ile-fed males (Supplementary Fig. 4f). There was no group effect in the total investigation time of the females (Supplementary Fig. 4j).

In the BMT, we observed an age-related deficit during the acquisition phase in both sexes, and while there was no significant effect of diet in either sex, aged low Ile-fed mice tended to perform more poorly than aged control-fed mice ($P = 0.28$ in males and $P = 0.11$ in females) (Fig. 2f,m). However, we noticed that some mice could quickly locate the escape box, ending the acquisition trial, but would then spend a notable amount of time hesitating instead of entering immediately. We manually measured this loitering time and found that loitering was persistent higher in low Ile-fed males and females and in low AA-fed females (Fig. 2g,n). In sharp contrast, young and aged control-fed mice of both sexes and low AA-fed males became increasingly decisive over the acquisition sessions (Fig. 2g,n).

https://doi.org/10.1038/s43587-024-00744-7

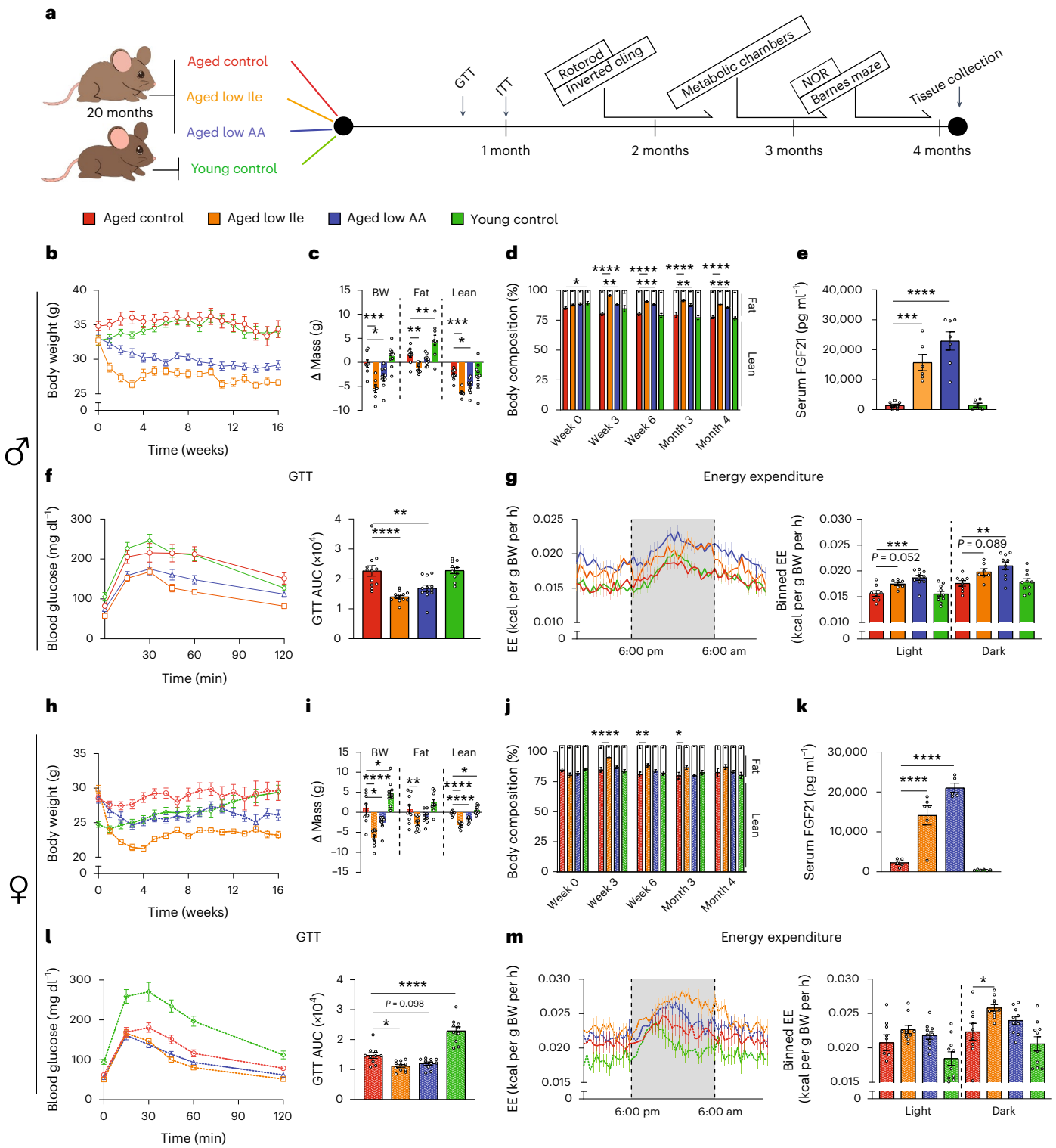


Fig. 1 | Low Ile and low AA diets promote leanness and metabolic health in aged mice. a, The experimental scheme. Three different AA-defined diets were utilized: control, low Ile and low AA. Aged mice began their respective diets at 20 months of age, while young mice were fed the control diet starting at 6 months of age. GTT, glucose tolerance test; ITT, insulin tolerance test. **b**, Male body weight changes over time for mice fed the indicated diets. **c**,**d**, The final changes in body weight (BW), fat mass and lean mass (**c**), as well as body composition for male mice fed the indicated diets (**d**). The *n* value varies over time, with maximum *n* = 12, 13, 12 and 10. **e**, Plasma FGF21 levels for male mice fed the indicated diets. *n* = 7, 6, 7 and 6. **f**, GTT in male mice fed the indicated diets. *n* = 12, 13, 12 and 10. **g**, Metabolic chambers were used to determine the energy expenditure (EE) of male mice. *n* = 8, 7, 10 and 10. The shaded period indicates the dark phase. **h**, Female body weight over time for mice fed the indicated diets. **i**,**j**, The final changes in body weight, lean mass and fat mass (**i**) and body composition (**j**) for female mice fed the indicated diets. The *n* value varies over time, with maximum *n* = 10, 11, 10 and 10. **k**, Plasma FGF21 for female mice fed the indicated diets. *n* = 5, 6, 5 and 6. **l**, GTT in female mice fed the indicated diets. *n* = 10, 11, 10 and 10. **m**, The energy expenditure of female mice. *n* = 9, 10, 10 and 10. The shaded period indicates the dark phase. The *n* values denote biologically independent animals and are listed in the order of aged control, aged low Ile, aged low AA and young control. *$P < 0.05$, **$P < 0.01$, ***$P < 0.001$ and ****$P < 0.0001$, ANOVA followed by two-sided Dunnett's test versus aged control-fed mice. Data are presented as mean ± s.e.m.

https://doi.org/10.1038/s43587-024-00744-7

Low Ile and low AA diets alter molecular indicators of aging

Recently, a panel of molecular indicators of aging rate that is remarkably conserved across multiple lifespan-extending treatments has been identified[20]. To determine the effect of late-life low Ile and low AA on these pathways, we analyzed tissues from mice fed these diets for 4 months at 24 months of age (Fig. 3a–i).

mTORC1 is a master regulator of growth and nutrient sensing, and is activated by BCAAs[21]. mTORC1 activity increases with age and its pharmacological inhibitor rapamycin is a robust geroprotector[22,23]. In the liver, we find that aged control-fed mice exhibit significantly higher levels of phosphorylated S6, a downstream mTORC1 readout, than young control-fed mice; this age-associated increase was suppressed in both aged low Ile- and low AA-fed animals (Fig. 3a,e). The phosphorylation of the mTORC1 substrate S6K1 was similarly suppressed by low AA in females ($P = 0.078$), but was unchanged in males. Phosphorylation of the mTORC1 substrate ULK1 S757 and the translation regulator eIF2α S51 was unchanged in all groups (Supplementary Fig. 5a–c). The expression of the mTORC1-controlled translation regulator 4E-BP1 was significantly decreased by aging in males, and this was increased by a low Ile diet and elevated by a low AA diet in males ($P = 0.19$). A similar trend was seen in females (Fig. 3a,e). The low Ile diet also suppressed the age-dependent increase in the phosphorylation of the mTORC2 target AKT S473 (Fig. 3a,e).

We further determined the phosphorylation status of S6 and AKT in the gastrocnemius muscle (Extended Data Fig. 3). We observed no effect of diet on S6 phosphorylation in aged males, while low Ile and low AA feeding in females suppressed S6 phosphorylation (Extended Data Fig. 3b,f). Neither males nor females showed any differences in AKT phosphorylation (Extended Data Fig. 3d,h).

The MAPK ERK signaling pathway regulates translation, increases with age and can be suppressed by the lifespan-extending treatments canagliflozin and 17aE2 (refs. 24,25). In the liver, the low Ile diet robustly decreased phosphorylation of the MAPK ERK pathway, while the effects of low AA was similar but less robust (Fig. 3b,f). An increase in cap-independent translation (CIT) is a shared feature in long-lived genetic and drug intervention models[26]. In the liver, aged control-fed mice had decreased CIT-related proteins compared with young control mice, which were reversed to various degrees by low Ile or low AA diets in both sexes (Fig. 3c,g). Finally, recent transcriptomic analysis has revealed that systemic shifts in fatty acid oxidation are associated with lifespan-extending interventions[27]. We identified age-dependent increases in the expression of several fatty acid regulators, such as fatty acid synthase (FASN), which were suppressed by both low Ile and low AA diets, with more consistent decreases induced by the former (Figs. 3d,h). Overall, both Low Ile and Low AA diets appear to induce molecular signatures that are similar to other life-extending interventions.

Low Ile diet induces hepatic transcriptomic adaptations

We performed transcriptional profiling of livers from aged control, aged low Ile and young control mice of both sexes. We identified differentially expressed genes (DEGs) induced by either old age and/or by diet. There were subtantially more DEGs found in females than males, but most of the diet-induced DEGs in males presented a greater degree of change (Extended Data Fig. 4a,b). In males, we identified 606 DEGs in response to aging (aged control versus young control) with 363 upregulated and 243 downregulated genes. For the diet effect, there were 125 DEGs between aged low Ile-fed and aged control-fed males, with 54 upregulated and 71 downregulated genes. In contrast, the females had 1,587 DEGs in response to aging, with 911 upregulated and 676 downregulated genes, and 2,379 DEGs responded to low Ile, with 1,257 upregulated and 1,122 downregulated genes. All DEGs induced by age and diet in both sexes are provided in Supplementary Table 1.

We then determined how the DEGs altered by age (aged control versus young control) are changed by diet in aged mice (aged control versus aged low Ile). Of the 363 DEGs upregulated in aged control-fed males, 354 became not significantly different and 4 became significantly downregulated in aged low Ile-fed males. Of the 243 DEGs downregulated in aged control-fed males, 220 became not significantly differently expressed and 2 became significantly upregulated in aged low Ile-fed males (Fig. 3j, left). A similar result was found in females. Of the 911 DEGs upregulated by age, the low Ile diet normalized the expression of 766, and 108 reversed to being downregulated. Of the 676 DEGs downregulated by age, the low Ile diet normalized the expression of 549 and 81 became upregulated (Fig. 3j, right). Overall, it seemed that the low Ile diet 'rejuvenates' the aging hepatic transcriptome in both sexes.

There was surprisingly little overlap between the male and female DEGs induced by a low Ile diet (Extended Data Fig. 5a), resulting in substantially different pathway enrichment in our Kyoto Encyclopedia of Genes and Genomes (KEGG) and Gene Ontology (GO) analysis (Extended Data Fig. 5b–i and Supplementary Tables 2 and 3). Using DEGs identified in each rejuvenation categories, we performed transcription factor enrichment using the Mining Algorithm for Genetic Controllers (Supplementary Table 4)[28]. The top 20 enriched transcription factors are displayed (Fig. 3k).

Low Ile and low AA diets induce hepatic senomorphic adaptations

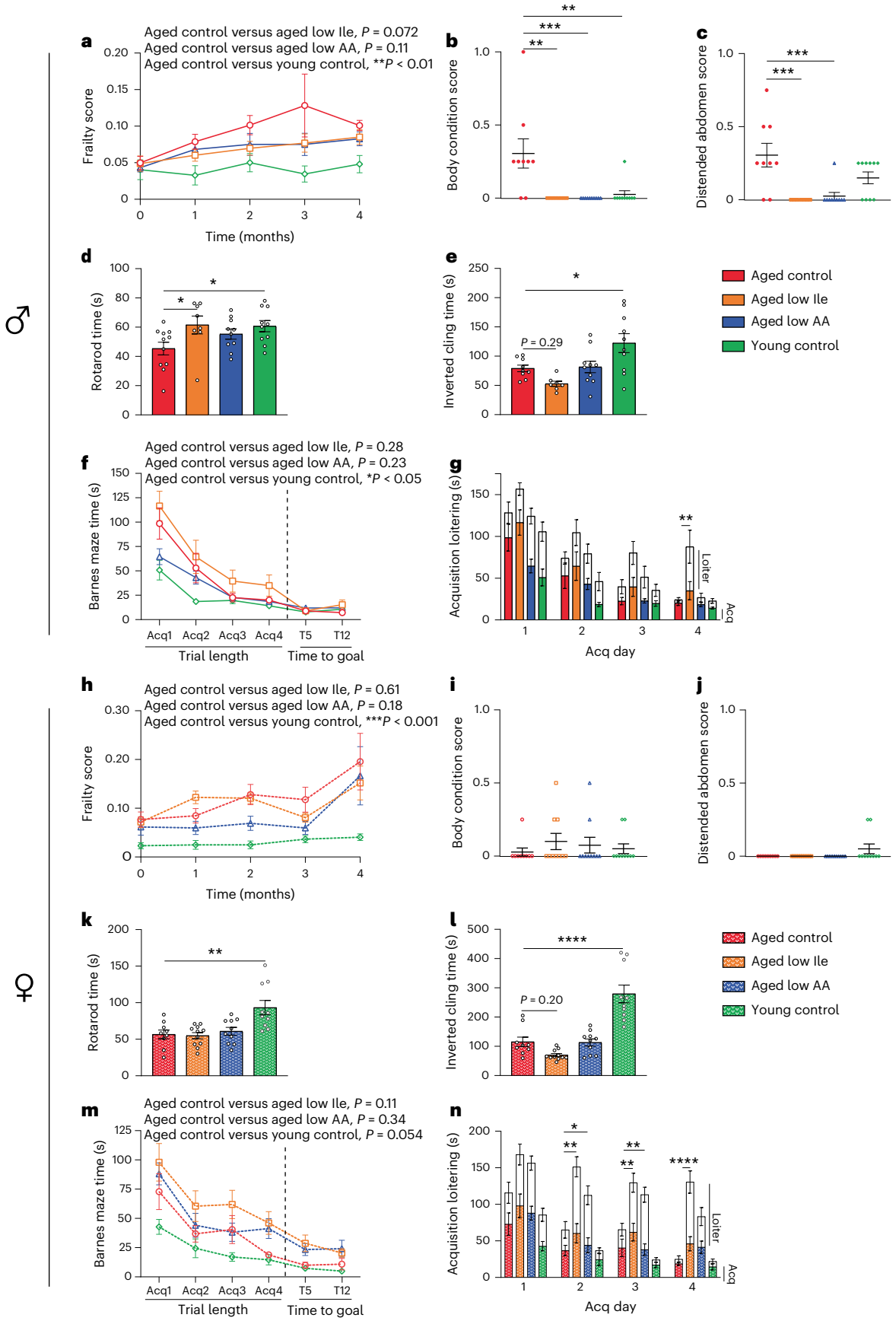
Cellular senescence plays a large role in promoting several aging phenotypes of the liver, including fibrosis and nonalcoholic fatty liver disease[29]. We performed quantitative PCR (RT–qPCR) to examine the gene expression of well-established senescence-associated markers in the livers of aged control-, low Ile- and low AA-fed males. Aged low Ile-fed males had significantly increased expression of *p21*, while low AA-fed males had significantly reduced expression of *Il-1α* and *Tnf-α* (Extended Data Fig. 6).

Low Ile and low AA diets induce changes in liver histology

We characterized how low Ile and low AA diets affect the histology of aged liver. First, hematoxylin and eosin (H&E) staining in males did not reveal any significant differences (Extended Data Fig. 7a–e). In females, the Nonalcoholic Fatty Liver Disease Activity Score (NAS)

Fig. 2 | Late-life feeding of low Ile and low AA diets promotes aspects of healthspan. a, The frailty score of male mice tracked between 20 and 24 months of age. The *n* value varies over time, with maximum $n = 12, 13, 12$ and 10. **b**,**c**, Male body condition (**b**) and distended abdomen frailty score (**c**), presented as the average of scores during the 3rd and 4th month of the experiment. $n = 9, 7, 10$ and 10. **d**,**e**, Male rotarod (**d**) and inverted cling performance (**e**) were assessed between 22 and 23 months of age. $n = 11, 8, 10$ and 10. **f**, The BMT performance of 24-month-old males with the indicated acquisition (Acq) trial days and test (T) trial days. **g**, The BMT acquisition trial duration with loitering of 24-month-old males. In **f** and **g**, $n = 8, 7, 10$ and 10. **h**, The frailty score of female mice tracked between 20 and 24 months of age. The *n* value varies over time, with maximum $n = 10, 11, 10$ and 10). **i**,**j**, Female body condition (**i**) and distended abdomen frailty score (**j**), presented as the average of scores during the 3rd and 4th month of the experiment. $n = 9, 10, 10$ and 10. **k**,**l**, Female rotarod (**k**) and inverted cling performance (**l**) were assessed between 22 and 23 months of age. $n = 9, 11, 10$ and 10. **m**, The BMT performance of 24-month-old females. **n**, The BMT acquisition trial duration with loitering of 24-month-old females. In **m** and **n**, $n = 8, 9, 9$ and 10. In **a** and **h**, a pairwise two-way mixed-effects analysis (REML) and in **f** and **m**, a two-way repeated measures ANOVA versus aged control-fed mice were performed. The *P* values represent the main effect of diet. In **b**–**e** and **i**–**l**, ANOVA followed by two-sided Dunnett's test versus aged control-fed mice and in **g** and **n**, the tests on loitering time only, ANOVA followed by two-sided Dunnett's test versus aged control-fed mice were performed. The *n* values denote biologically independent animals and are listed in the order of aged control, aged low Ile, aged low AA and young control. $^{*}P < 0.05$, $^{**}P < 0.01$, $^{***}P < 0.001$ and $^{****}P < 0.0001$. Data presented as mean ± s.e.m.

https://doi.org/10.1038/s43587-024-00744-7



https://doi.org/10.1038/s43587-024-00744-7

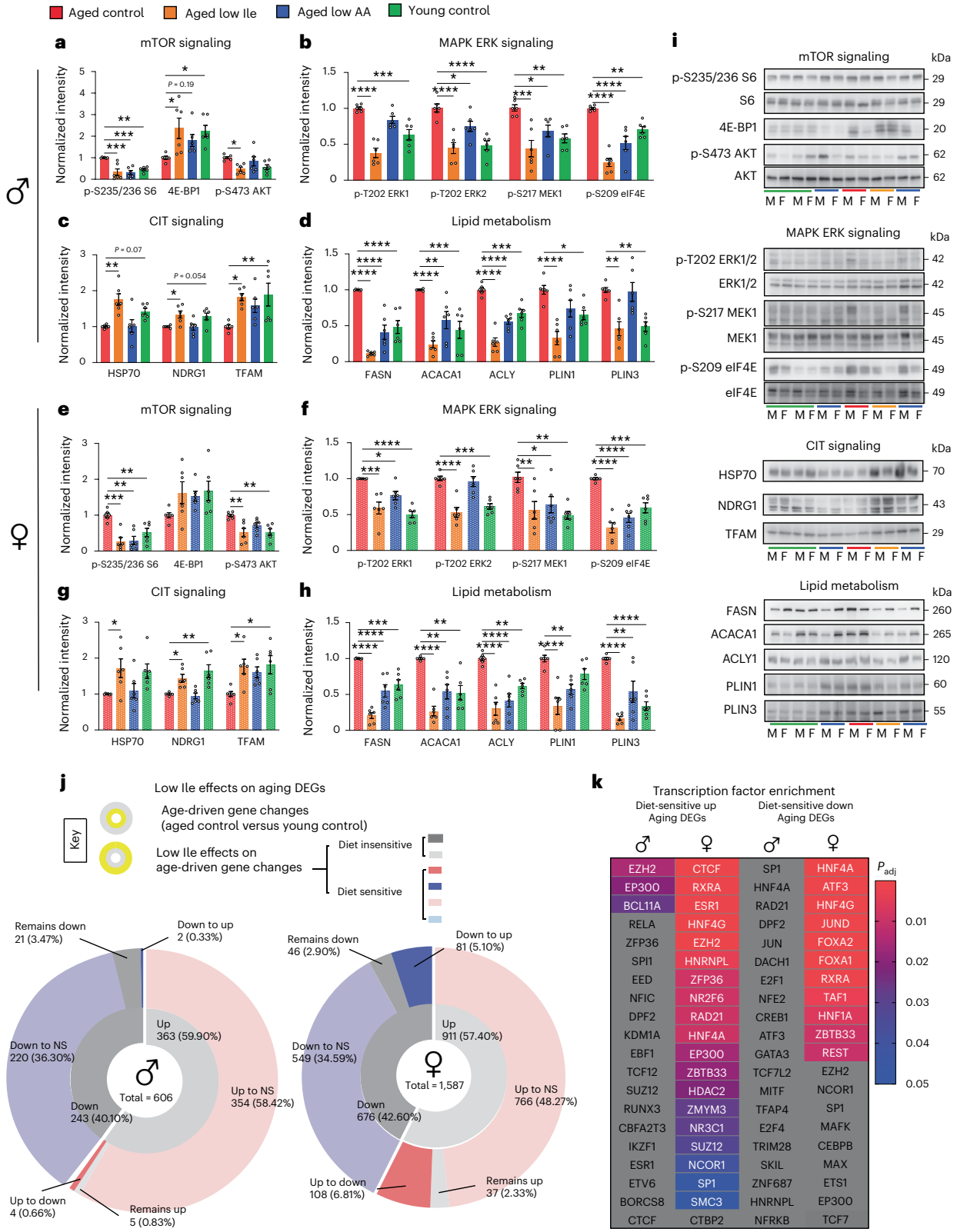


Fig. 3 | Low Ile and low AA diet ameliorates multiple molecular indicators of aging rate in the liver. a–**d**, Diet and age alters aging rate indicators related to mTOR signaling (**a**), MAPK ERK signaling (**b**), CIT (**c**) and lipid oxidation (**d**) in the liver of male mice. **e**–**h**, Diet and age alters aging rate indicators related to mTOR signaling (**e**), MAPK ERK signaling (**f**), CIT (**g**) and lipid oxidation (**h**) in the liver of female mice. **i**, Representative western blots of the analyzed proteins in males (M) and females (F). In **a**–**i**, $n = 6$ biologically independent animals/group, ANOVA followed by two-sided Dunnett's test. $^{*}P < 0.05$, $^{**}P < 0.01$, $^{***}P < 0.001$ and $^{****}P < 0.0001$. Data are presented as mean ± s.e.m. **j**, A summary of the effect of low Ile on the age-driven DEG sets in males (left) and females (right). The inner ring represents the genes up- or downregulated by aging, while the outer ring represents the effect of a low Ile diet on the DEGs altered with aging. $n = 5$ (female, aged low Ile) and 6 (all other groups) biologically independent animals. **k**, Mining Algorithm for Genetic Controllers transcription factor enrichment analysis, with the top 20 results from each rejuvenation category. DEGs were identified using an empirical Bayes moderated linear model, and log coefficients and Benjamini–Hochberg-adjusted P values (P_{adj}) were generated for each comparison of interest ($\alpha = 0.10$).

https://doi.org/10.1038/s43587-024-00744-7

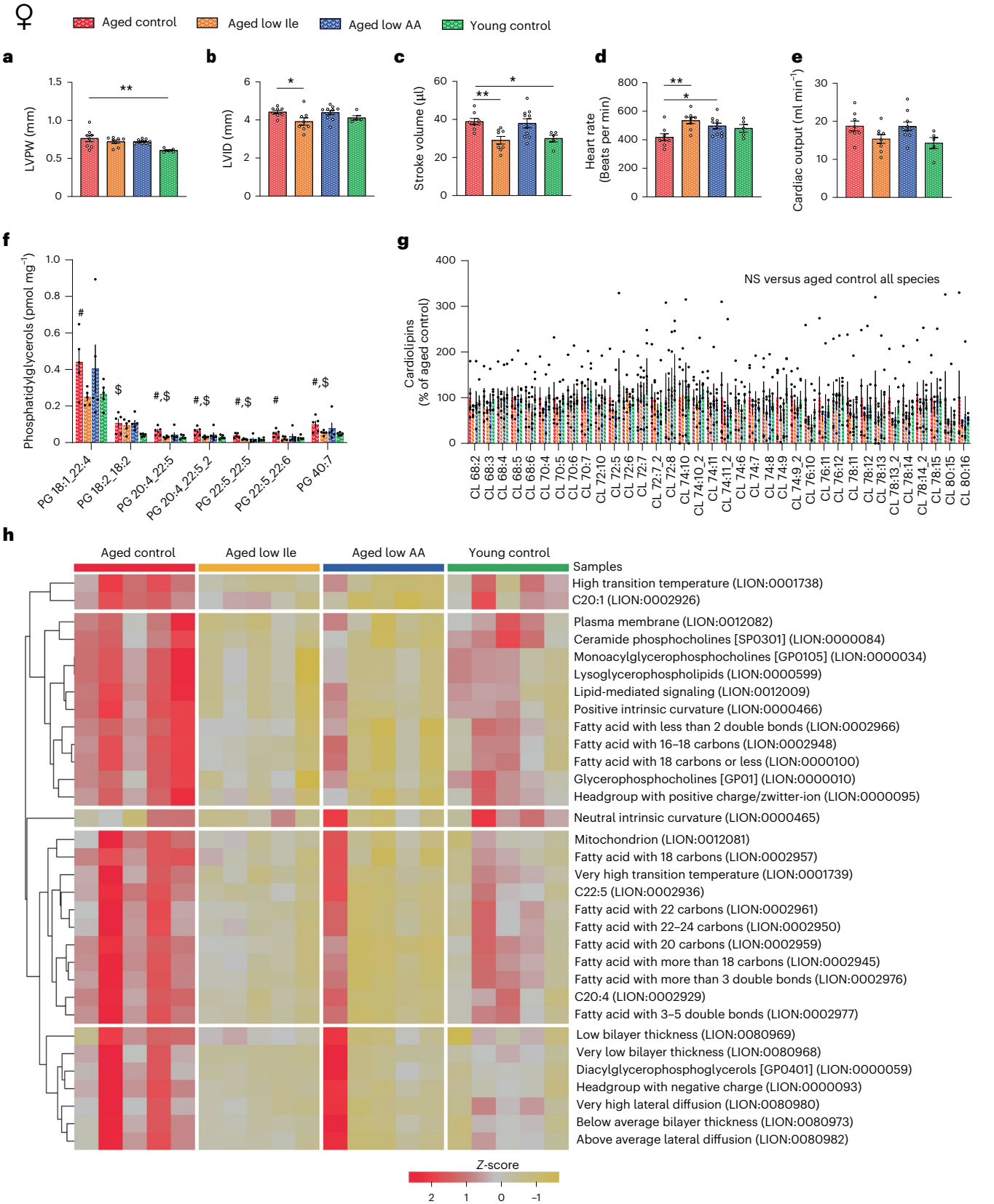


Fig. 4 | Low Ile diet promotes youthful functional and molecular aspects of the female mice heart. a–**e**, Echocardiogram evaluation of female mice at 25 months of age measuring LV posterior wall diameter (LVPW) (**a**), LV inner diameter (LVID) (**b**), stroke volume (**c**), heart rate (**d**) and cardiac output (**e**). $n = 6, 7, 5$ and 5. $^{*}P < 0.05$ and $^{**}P < 0.01$, ANOVA followed by two-sided Dunnett's test. **f**,**g**, Statistically significant phosphatidylglycerols (PG) (**f**) and all cardiolipins (CL) (**g**) in female mice hearts at 24 months of age after 4 months of dietary intervention. $n = 8, 8, 10$ and 5, $^{\#}P < 0.05$ aged control versus aged low Ile, $^{\$}P < 0.05$ aged control versus young control, two-tailed t-test. NS, not significant. **h**, LION lipid ontology analysis of significantly altered lipid species in the female mice heart. The n values denote biologically independent animals and are listed in the order of aged control, aged low Ile, aged low AA and young control. Data are presented as mean ± s.e.m.

score was significantly increased in aged low Ile-fed mice, mostly induced by lobular inflammation (Extended Data Fig. 7f,h). Aged low AA-fed females had an increase in steatosis (Extended Data Fig. 7g). F4/80 staining for macrophage proliferation in aged low Ile-fed females was increased, correlating with the increased H&E score for lobular inflammation (Extended Data Fig. 7j–m). Oil red O staining for lipid droplets did not find any significant differences between groups (Extended Data Fig. 8a–e). Sirius red staining to highlight the birefringence of hepatic collagen fibers showed that aged low Ile-fed males had significantly higher fibrosis (Extended Data Fig. 8f,g). On the other hand, while none of the female mice liver fibrosis scores were significantly different from the aged control-fed mice, the baseline score of females were overall higher than that of males (Extended Data Fig. 8g,h).

Low Ile diet induces sex-specific cardiac remodeling

We performed echocardiography to evaluate heart function in a separate cohort of animals at 25 months of age after 6 weeks of dietary intervention. We identified a number of sex-specific and diet-induced cardiac effects (Fig. 4 and Extended Data Table 2). In aged males, the low Ile diet increased left ventricular (LV) mass while decreasing mean and peak aortic flow velocity relative to aged control-fed males (Extended Data Table 2). In contrast, we detected an age-dependent increase in the LV posterior wall thickness and the stroke volume of aged control-fed females (Fig. 4a,c). Aged low Ile-fed females had a significant decrease in diastolic LV inner diameter, decreased stroke volume and increased heart rate relative to aged control-fed females; Aged low AA-fed females showed only an increase in heart rate (Fig. 4b–d). There were no significant changes in cardiac output in either sex (Extended Data Table 2 and Fig. 4e).

We performed lipidomic profiling on the hearts of female mice collected at 24 months of age following 4 months of dietary intervention. We observed significant age-dependent increases in several phosphatidylglycerol species that were ameliorated in the low Ile-fed mice (Fig. 4f). As phosphatidylglycerol is the primary component of the mitochondrial outer membrane, we also explored the most abundant mitochondrial inner membrane lipid and the phosphatidylglycerol derivative, cardiolipin. Interestingly, all cardiolipin species were unchanged (Fig. 4g); the increase in phosphatidylglycerol without a change in cardiolipins could indicate a shift in mitochondrial morphology and increased fission[30]. We performed lipid ontology enrichment analysis (LION) using all significantly altered lipid species (Fig. 4h). Overall, we observed a rejuvenating effect on the lipid profile of both low Ile- and Low AA-fed females. The list of all differentially expressed lipid species are provided in Supplementary Table 5.

Discussion

Recent work from our laboratory and others has demonstrated that calorie quality, not just total quantity, is a critical determinant of biological health. Reducing dietary levels of protein, the three BCAAs or isoleucine alone improves metabolic health and extends the lifespan of young mice[4,6,10,14,15]. Here, we began to determine whether these benefits hold true in aged mice using a previously proposed phenotyping pipeline[31]. Starting low Ile and low AA diets in mice at 20 months of age, roughly equivalent to 60 years of age in a human, we found that many of the metabolic benefits are similar to those we observed in younger animals. In particular, low Ile and low AA diets have dramatic and largely positive effects on weight, body composition, glycemic control and energy balance.

There are several challenges that limit the interpretation of these results. Any change in dietary composition necessarily reflects tradeoffs with other macronutrients to keep the diets isocaloric. The low AA diet increases the level of carbohydrates as well as the ratio between carbohydrates and protein, which may contribute to the overall biological response. The low Ile diet keeps carbohydrates constant, but increases the levels of several nonessential AAs slightly to maintain the calorie contribution from AAs as well as overall nitrogen level; however, as isoleucine is relatively low in abundance in these diets to begin with, a 67% decrease in Ile involves only a very small compensatory increase in other AAs.

Malnutrition, including that of dietary protein, has been recognized as a major health concern in aging adults as it could potentially increase the risk for multiple diseases including sarcopenia[32]. However, it has been challenging to prove this; for example, it appears that protein supplementation improves lean mass and function in older humans with sarcopenia but not in healthy older adults[33], and a recent UK-based twin study concluded that protein intake is positively associated with sarcopenia[34]. Thus, research remains to be done to determine how the results shown here can be safely translated to older humans.

A key driver of sarcopenia may be hyperactive mTORC1 in the muscle or at the neuromuscular junction[22,35,36]. Here, a low AA diet was able to suppress hyperactive muscle mTORC1 activity in females. Nevertheless, we observed a rapid loss of lean mass induced by both diets in aged mice, which is in contrast with our previous findings in young mice. Additionally, our frailty data suggest that low Ile and low AA diets may help slow select, but not all, age-associated deficits. In the evaluation of cognitive performance, we were unable to discern benefits elicited by either diet, which is at odds with previous findings in Alzheimer's disease mice[37,38]. The effects of these diets on cardiac health appear to also be mixed. Larger cohorts studied for a longer period will be required to reach more definitive answers on the optimal protein and isoleucine intake to maximize late-life healthspan.

The low Ile and the low AA diet had similar rejuvenating effects on multiple molecular aging rate indicators, effectively phenocopying several bona fide lifespan-extending treatments and genetic models. Senescence markers in the liver were sensitive to the diets, with low AA generally eliciting a beneficial suppression of *Il1-α* and *Tnf-α* expression, while low Ile appears to increase *p21* expression. We found increased macrophages in the livers of aged low Ile-fed females, indicating possible interactions with the immune system. Finally, taking an unbiased global approach, we find that a low Ile diet reverses most age-related changes in the hepatic transcriptome in both sexes. Overall, these data suggest that at the molecular level, a low Ile or a low AA diet have many beneficial, perhaps rejuvenating, molecular effects in aged mice. While the feasibility and the efficacy of restricting protein or isoleucine intake clinically are unknown, our findings here suggest that it may never be too late to reap the benefits of switching to a low-protein or an isoleucine-restricted diet.

Methods

Animals

All procedures were performed in accordance to institutional guidelines and were approved by the Institutional Animal Care and Use Committee of William S. Middleton Memorial Veterans Hospital. C57BL/6J.Nia mice from the NIA aged rodent colony were obtained at 6, 20 or 24 months of age as indicated. Mice were housed as shipped, with groups of four or more split into groups of two to three animals per cage. Animals were provided ad libitum access to Laboratory Rodent Diet 5001 diet for 1–2 weeks before beginning their respective dietary interventions. All mice were maintained at a temperature of approximately 22 °C and health checks were performed daily by the facility staff. Relative humidity of the animal room ranges between 30% and 70%, with an average of 42%. Mice were housed in a specific pathogen-free facility in static microisolator cages under 12:12 light cycle conditions with ad libitum access to food and water unless specified below for upcoming experiments.

No formal method of randomization was used but aged mice were allocated at the cage level to reach comparable body weight, body composition and frailty scores between groups. The diet groups were as follows: control with 21% calories derived from AAs (TD.140711, Envigo), low Ile with 67% less isoleucine content than the control

diet (TD.160734) and low AA diets with 7% calories derived from AAs (TD.140714). The three diets are isocaloric, with nonessential AAs increased to balance calories in the low Ile diet and carbohydrates increased to balance calories in the low AA diet. The full composition of these diets is provided in Extended Data Table 1.

Metabolic chamber indirect calorimetry was carried out using an Oxymax/CLAMS-HC metabolic chamber system (Columbus Instruments) for ~48 continuous hours. The first ~24 h of data were discarded as the acclimation period with a subsequent continuous 24 h period utilized for data analysis. Food consumption monitoring was carried out in home cages over 2–4 days and analyzed using the total animal mass in the cage. Body composition was determined using an EchoMRI body composition analyzer.

In vivo procedures

Glucose and insulin tolerance tests were performed by fasting the mice overnight for 16 h or 4 h in the morning, respectively. In respective tests, mice were injected with glucose (1 g kg^{-1}; Sigma, G7021) or insulin (0.75 U kg^{-1}; Novolin) intraperitoneally. Blood glucose was monitored via a Bayer Contour glucometer and test strips (Bayer). All behavior tracking was done automatically with the EthoVision XT program (Noldus). All following behavior/fitness testing followed previously described protocols[31].

NOR. Briefly, the habituation/open field test was followed by the acquisition trial. The short-term memory test was carried out 1 h after the acquisition trial, and the long-term memory test was carried out at 23 h after the acquisition trial. The habituation, acquisition and short- and long-term memory test were 5 min each.

BMT. Briefly, the test was carried out on a maze table with 20 possible exit holes with distinct visible landmarks outside of the arena. Each animal was exposed to four acquisition days with a maximum trial time of 180 s. On day 5, a test trial takes place for short-term memory; then the mice are not experimented with until day 12, when a long-term memory test trial takes place.

Rotarod. Animals were trained on a slow-moving rotarod at 4 rpm. On test trials, the accelerating rotarod (Rotamex 5, Columbus Instruments) was set to increase by 0.5 rpm per 4 s. There was a minimum rest period of 30 min between training and trials for each animal. The average trial performance for three test trials was taken for statistical analysis.

Inverted cling. Animals were placed onto a wire grid bounded with masking tape and inverted onto the test bin. Mice naive to the experiment are first trained through three trials of 30 s gripping before test trials. There was a minimum of 30 min rest between training, and for each animal, three test trials were averaged for analysis.

Echocardiogram. Mice used for echocardiography were separate from the main study at a later age as indicated. Transthoracic echocardiography was performed using a Visual Sonics Vevo 770 ultrasonograph with a 30 MHz transducer as detailed previously[10,39]. For acquisition of two-dimensional guided M-mode images at the tips of papillary muscles and Doppler studies, mice were sedated with 1% isoflurane administered through a facemask with hair removed, and maintained on a heated platform. Blood velocities across the mitral, aortic and pulmonary valves were measured using Doppler pulsed-wave imaging, angling the probe to obtain a nearly parallel orientation to the blood flow. End diastolic and systolic LV diameter, as well as anterior and posterior wall (AW and PW, respectively) thickness were measured on line from M-mode images obtained in a parasternal long-axis view using the leading-edge-to-leading-edge convention. All parameters were measured over at least three consecutive cardiac cycles and averaged. LV fractional shortening was calculated as $((\text{LV diameter}_{\text{diastolic}} - \text{LV diameter}_{\text{systolic}})/\text{LV diameter}_{\text{diastolic}}) \times 100$; ejection fraction: $((7.0/(2.4 + \text{LV diameter}_{\text{diastolic}})(\text{LV diameter}_{\text{diastolic}})3 - (7.0/(2.4 + \text{LV diameter}_{\text{systolic}})(\text{LV diameter}_{\text{systolic}})3/(7.0/(2.4 + \text{LV diameter}_{\text{diastolic}})(\text{LV diameter}_{\text{diastolic}})3 \times 100$; and LV mass: $(1.05 \times ((\text{PW}_{\text{diastolic}} + \text{AW}_{\text{diastolic}} + \text{LV diameter}_{\text{diastolic}})3 - (\text{LV diameter}_{\text{diastolic}})3))$. Heart rate was determined from at least three consecutive intervals from the pulsed-wave Doppler tracings of the LV outflow tract. Ejection time was measured from the same outflow track tracings from the onset of flow to the end of flow. Isovolumic relaxation time was measured as the time from the closing of the aortic valve to the opening of the mitral valve from pulsed-wave Doppler tracings of the LV outflow tract and mitral inflow region. The same investigator obtained all images and measures.

FGF21 enzyme-linked immunosorbent assay. Circulating FGF21 was measured using blood plasma obtained after 16 h overnight fast and 3 h refeed at 4 months after diet start, age 24 months for aged mice and age 10 months for young adult mice. Circulating FGF21 was quantified using a mouse/rat FGF21 quantikine enzyme-linked immunosorbent assay kit (MF2100, R&D Systems).

Western blots. Mice were euthanized after overnight fasting and then refeeding all mice for 3–4 h with their respective diets. All tissues were flash frozen in liquid nitrogen. Liver lysate was homogenized in RIPA buffer with EDTA-free Protease and Phosphotase Inhibitor Mini Tablet (Thermo Scientific, A32961). Each phosphoresidue was normalized to the loading control and then normalized to its total protein before being expressed as a ratio of the aged control. Primary antibodies are utilized between 1:1,000 and 1:500 dilution. Antibody product codes are provided in Supplementary Table 6.

RT–qPCR. RT–qPCR was carried out according to protocols described previously[40] using TRI Reagent according to the manufacturer's protocol. The primers that were used are as follows are listed in Supplementary Table 6.

Heart lipidomics. Methyl-*tert*-butyl ether extraction was performed with standards from SPLASH Lipidomix from Avanti, using methods outlined previously[41]. Signal from the processed blank was subtracted as background during data processing. For positive mode, samples were diluted to 15× in MeOH and 3 µl was injected. Samples were run undiluted in negative mode and 5 µl were injected. Tandem mass spectrometry data from pooled samples were run through Agilent LipidAnnotator and then used to process mass spectrometry 1 data with Profinder (v8.0). Data were normalized to the internal standards and tissue weight and further processed using R.

Liver histology

After euthanasia, a portion of each liver was placed into optimal cutting temperature compound and frozen on dry ice for later histological analysis. For the scoring of the H&E staining and the Sirius red staining, a blinded evaluator scored the sections three times and the average score for each animal was taken for statistical analysis. For each mice, two to four fields of view were taken for quantification. Images of the H&E-stained liver was scored using the NAS. Briefly, the three categories of the NAS score are as follows: steatosis (0–3), from <5% to >66% of surface area involved by steatosis; lobular inflammation (0–3), from no inflammatory foci to >4 inflammatory foci per 200 × 200 area; and hepatocyte ballooning (0–2), from none to many prominent ballooning cells. Fibrosis stage scoring of the Sirius red-stained collagen fibers was done through birefringence visualization under polarized microscopy of the entire section. Images provided are representative areas. Briefly, fibrosis stage scoring was as follows: (0) no fibrosis, (1) slight perisinusoidal or periportal fibrosis, (2) perisinusoidal and portal/periportal fibrosis, (3) bridging

fibrosis or (4) clear cirrhosis. The antibodies used are listed in Supplementary Table 6.

Statistics and reproducibility

All statistical analyses were conducted using Prism, version 9 (GraphPad Software Inc.). Tests involving multiple factors were analyzed by either a two-way analysis of variance (ANOVA) with time and group as categorical variables or by one-way ANOVA with group as the categorical variable followed by a two-sided Dunnett's post hoc test for multiple comparisons against the aged control. Where measurements were taken longitudinally, a mixed-effects model (REML) or two-way repeated-measures ANOVA was used. Energy expenditure data were analyzed by linear regression of energy expenditure by body weight (analysis of covariance). The sample sizes for metabolic studies were determined based on our previously published experimental results regarding the effects of low Ile diet feeding[13], with the goal of having >90% power to detect a change in the area under the curve (AUC) during a glucose tolerance tests (GTT) ($P < 0.05$). Data distribution was assumed to be normal but this was not formally tested.

Blinding. As the diets were colored and the young/old animals can be easily differentiated, data collection and analysis were not performed blind to the condition of the experiments.

Randomization. No formal method of randomization was used but aged mice were allocated at the cage level to reach comparable body weight, body composition and frailty scores between groups.

Data exclusion. For the transcriptomic dataset, one animal was excluded after exploratory analysis due to being a notable outlier on principal component analysis. However, the full dataset is provided in the repository.

Transcriptomic analysis

RNA was extracted from the liver using the PureLink RNA mini kit (Invitrogen, 12183025) with DNase (Invitrogen, 12185010). The concentration and purity of RNA was determined using a NanoDrop 2000c spectrophotometer (Thermo Fisher Scientific) and RNA was diluted to 100–400 ng μl^{-1}. The RNA was submitted to the University of Wisconsin–Madison Biotechnology Center Gene Expression Center and DNA Sequencing Facility, and RNA quality was assayed using an Agilent RNA NanoChip. RNA libraries were prepared using the TruSeq Stranded Total RNA Sample Preparation protocol (Illumina) with 250 ng of messenger RNA, and cleanup was done using RNA clean beads. Reads were aligned to the mouse (*Mus musculus*) with genome-build GRCm38.p5 of accession NCBI:GCA_000001635.7 and expected counts were generated with ensembl gene IDs[42].

Analysis of significantly DEGs was completed in R version 4.2.285 using edgeR[43] and limma[44]. Gene names were converted to gene symbol and Entrez ID formats using the mygene package. Males and females were analyzed separately, with one female outlier removed following principal component analysis analysis of the raw data. To reduce the impact of external factors not of biological interest that may affect expression, data were normalized to ensure the expression distributions of each sample were within a similar range. We normalized using the trimmed mean of *M*-values, which scales to library size. Heteroscedasticity was accounted for using the voom function, DEGs were identified using an empirical Bayes moderated linear model and log coefficients and Benjamini–Hochberg-adjusted *P* values were generated for each comparison of interest ($\alpha = 0.10$). DEGs were used to identify enriched pathways, both GO and Kyoto Encyclopedia of Genes and Genomes enriched pathways were determined for each contrast, with significantly enriched DEGs (false discovery rate cutoff of 0.1, $\alpha = 0.05$). All GO categories (cellular component, biological process and molecular function) are presented together.

Reporting summary

Further information on research design is available in the Nature Portfolio Reporting Summary linked to this article.

Data availability

RNA sequencing data have been deposited with Gene Expression Omnibus, accession GSE254721. Heart lipidomics data have been deposited with MassIVE, identifier MSV000095324. The data that support the plots within this article and other findings of this study, including full scans of western blot images, are provided as Source data files. All data supporting the findings of the study are available from the corresponding author upon request. Source data are provided with this paper.

References

1. Mihaylova, M. M. et al. When a calorie is not just a calorie: diet quality and timing as mediators of metabolism and healthy aging. *Cell Metab.* **35**, 1114–1131 (2023).
2. Levine, M. E. et al. Low protein intake is associated with a major reduction in IGF-1, cancer, and overall mortality in the 65 and younger but not older population. *Cell Metab.* **19**, 407–417 (2014).
3. Sluijs, I. et al. Dietary intake of total, animal, and vegetable protein and risk of type 2 diabetes in the European Prospective Investigation into Cancer and Nutrition (EPIC)-NL study. *Diabetes Care* **33**, 43–48 (2010).
4. Fontana, L. et al. Decreased consumption of branched-chain amino acids improves metabolic health. *Cell Rep.* **16**, 520–530 (2016).
5. Ferraz-Bannitz, R. et al. Dietary protein restriction improves metabolic dysfunction in patients with metabolic syndrome in a randomized, controlled trial. *Nutrients* **14**, 2670 (2022).
6. Solon-Biet, S. M. et al. The ratio of macronutrients, not caloric intake, dictates cardiometabolic health, aging, and longevity in ad libitum-fed mice. *Cell Metab.* **19**, 418–430 (2014).
7. Mair, W., Piper, M. D. & Partridge, L. Calories do not explain extension of life span by dietary restriction in *Drosophila*. *PLoS Biol.* **3**, e223 (2005).
8. Solon-Biet, S. M. et al. Dietary protein to carbohydrate ratio and caloric restriction: comparing metabolic outcomes in mice. *Cell Rep.* **11**, 1529–1534 (2015).
9. Hill, C. M. et al. FGF21 is required for protein restriction to extend lifespan and improve metabolic health in male mice. *Nat. Commun.* **13**, 1897 (2022).
10. Richardson, N. E. et al. Lifelong restriction of dietary branched-chain amino acids has sex-specific benefits for frailty and lifespan in mice. *Nat. Aging* **1**, 73–86 (2021).
11. White, P. J. et al. Branched-chain amino acid restriction in Zucker-fatty rats improves muscle insulin sensitivity by enhancing efficiency of fatty acid oxidation and acyl-glycine export. *Mol. Metab.* **5**, 538–551 (2016).
12. Cummings, N. E. et al. Restoration of metabolic health by decreased consumption of branched-chain amino acids. *J. Physiol.* **596**, 623–645 (2018).
13. Yu, D. et al. The adverse metabolic effects of branched-chain amino acids are mediated by isoleucine and valine. *Cell Metab.* **33**, 905–922.e6 (2021).
14. Solon-Biet, S. M. et al. Branched chain amino acids impact health and lifespan indirectly via amino acid balance and appetite control. *Nat. Metab.* **1**, 532–545 (2019).
15. Green, C. L. et al. Dietary restriction of isoleucine increases healthspan and lifespan of genetically heterogeneous mice. *Cell Metab.* **35**, 1976–1995.e6 (2023).
16. Deelen, J. et al. A metabolic profile of all-cause mortality risk identified in an observational study of 44,168 individuals. *Nat. Commun.* **10**, 3346 (2019).
17. Hahn, O. et al. A nutritional memory effect counteracts benefits of dietary restriction in old mice. *Nat. Metab.* **1**, 1059–1073 (2019).

18. Flurkey, K., Currer, J. & Harrison, D. in *The Mouse in Biomedical Research* 2nd edn (ed. Fox, J. G.) 637–672 (American College Laboratory Animal Medicine, 2007).
19. Whitehead, J. C. et al. A clinical frailty index in aging mice: comparisons with frailty index data in humans. *J. Gerontol. A* **69**, 621–632 (2014).
20. Miller, R. A., Li, X. & Garcia, G. Aging rate indicators: speedometers for aging research in mice. *Aging Biol.* https://doi.org/10.59368/agingbio.20230003 (2023).
21. Simcox, J. & Lamming, D. W. The central moTOR of metabolism. *Dev. Cell* **57**, 691–706 (2022).
22. Baar, E. L., Carbajal, K. A., Ong, I. M. & Lamming, D. W. Sex- and tissue-specific changes in mTOR signaling with age in C57BL/6J mice. *Aging Cell* **15**, 155–166 (2016).
23. Mannick, J. B. & Lamming, D. W. Targeting the biology of aging with mTOR inhibitors. *Nat. Aging* **3**, 642–660 (2023).
24. Jiang, E., Dinesh, A., Jadhav, S., Miller, R. A. & Garcia, G. G. Canagliflozin shares common mTOR and MAPK signaling mechanisms with other lifespan extension treatments. *Life Sci.* **328**, 121904 (2023).
25. Miller, R. A. et al. Canagliflozin extends life span in genetically heterogeneous male but not female mice. *JCI Insight* **5**, e140019 (2020).
26. Shen, Z., Hinson, A., Miller, R. A. & Garcia, G. G. Cap-independent translation: a shared mechanism for lifespan extension by rapamycin, acarbose, and 17α-estradiol. *Aging Cell* **20**, e13345 (2021).
27. Watanabe, K. et al. Lifespan-extending interventions induce consistent patterns of fatty acid oxidation in mouse livers. *Commun. Biol.* **6**, 768 (2023).
28. Roopra, A. MAGIC: a tool for predicting transcription factors and cofactors driving gene sets using ENCODE data. *PLoS Comput. Biol.* **16**, e1007800 (2020).
29. Matthew, S. et al. in *Hepatocellular Carcinoma* (eds Streba, C. T., Vere, C. C. & Rogoveanu, I.) Ch. 4 (IntechOpen, 2017).
30. Dorn, G. Mitochondrial fission/fusion and cardiomyopathy. *Curr. Opin. Genet. Dev.* **38**, 38–44 (2016).
31. Bellantuono, I. et al. A toolbox for the longitudinal assessment of healthspan in aging mice. *Nat. Protoc.* **15**, 540–574 (2020).
32. Norman, K., Haß, U. & Pirlich, M. Malnutrition in older adults-recent advances and remaining challenges. *Nutrients* **13**, 2764 (2021).
33. Nasimi, N. et al. Whey protein supplementation with or without vitamin D on sarcopenia-related measures: a systematic review and meta-analysis. *Adv. Nutr.* **14**, 762–773 (2023).
34. Ni Lochlainn, M., Bowyer, R. C. E., Welch, A. A., Whelan, K. & Steves, C. J. Higher dietary protein intake is associated with sarcopenia in older British twins. *Age Ageing* **52**, afad018 (2023).
35. Castets, P., Ham, D. J. & Rüegg, M. A. The TOR pathway at the neuromuscular junction: more than a metabolic player? *Front. Mol. Neurosci.* **13**, 162 (2020).
36. Joseph, G. A. et al. Partial inhibition of mTORC1 in aged rats counteracts the decline in muscle mass and reverses molecular signaling associated with sarcopenia. *Mol. Cell. Biol.* **39**, e00141–19 (2019).
37. Tournissac, M. et al. Dietary intake of branched-chain amino acids in a mouse model of Alzheimer's disease: effects on survival, behavior, and neuropathology. *Alzheimers Dement.* **4**, 677–687 (2018).
38. Babygirija, R. et al. Protein restriction slows the development and progression of pathology in a mouse model of Alzheimer's disease. *Nat. Commun.* **15**, 5217 (2024).
39. Harris, S. P. et al. Hypertrophic cardiomyopathy in cardiac myosin binding protein-C knockout mice. *Circ. Res.* **90**, 594–601 (2002).
40. Calubag, M. F. et al. FGF21 has a sex-specific role in calorie-restriction-induced beiging of white adipose tissue in mice. *Aging Biol.* **1**, 3 (2022).
41. Jain, R., Wade, G., Ong, I., Chaurasia, B. & Simcox, J. Determination of tissue contributions to the circulating lipid pool in cold exposure via systematic assessment of lipid profiles. *J. Lipid Res.* **63**, 100197 (2022).
42. Zerbino, D. R. et al. Ensembl 2018. *Nucleic Acids Res.* **46**, D754–D761 (2017).
43. Robinson, M. D., McCarthy, D. J. & Smyth, G. K. edgeR: a Bioconductor package for differential expression analysis of digital gene expression data. *Bioinformatics* **26**, 139–140 (2010).
44. Ritchie, M. E. et al. limma powers differential expression analyses for RNA-sequencing and microarray studies. *Nucleic Acids Res.* **43**, e47 (2015).

Acknowledgements

We thank J. Chen and J. Berg at the University of Michigan for assistance with molecular analysis of tissues, as well as all members of the Lamming laboratory for their assistance and input. The Lamming laboratory is supported in part by the National Institutes of Health (NIH)/NIA (AG056771, AG062328, AG081482, AG084156 and AG085898 to D.W.L.), National Institute of Health/National Institute of Diabetes and Digestive and Kidney Diseases (DK125859 to D.W.L.) and startup funds from the University of Wisconsin–Madison School of Medicine and Public Health and Department of Medicine to D.W.L. C.-Y.Y. was supported in part by a training grant (T32AG000213), a National Institute of Aging F32 postdoctoral fellowship (F32AG077916) and a National Institute of Aging K99 award (K99AG084921). M.F.C. is supported by F31AG082504. R.B. is supported by F31AG081115. M.E.T. is supported by F99AG083290. C.L.G. is supported by HF AGE-009 from the Hevolution Foundation. M.M.S. is supported in part by a Supplement to Promote Diversity in Health-Related Research RF1AG056771-06S1. H.H.P. is supported in part by F31AG066311. J.A.S. is supported by the National Institute of Diabetes and Digestive and Kidney Diseases (R01DK133479) and Juvenile Diabetes Research Foundation (JDRF201309442) and J.W.D. is supported by an National Science Foundation Graduate Research Fellowship Program. J.A.S. is a Howard Hughes Medical Institute Freeman Hrabowski Scholar and is an American Federation for Aging Research grant recipient (A22068). R.A.M. and G.G.G. are supported by the Glenn Foundation for Medical Research. Support for this research was provided by the University of Wisconsin–Madison Office of the Vice Chancellor for Research and Graduate Education with funding from the Wisconsin Alumni Research Foundation. The authors used the University of Wisconsin–Madison Biotechnology Center Gene Expression Center (RRID:SCR_017757) and the University of Wisconsin Carbone Cancer Center Experimental Animal Pathology Laboratory (P30CA014520). The Lamming laboratory was supported in part by the US Department of Veterans Affairs (I01-BX004031 and IS1-BX005524), and this work was supported using facilities and resources from the William S. Middleton Memorial Veterans Hospital. The content is solely the responsibility of the authors and does not necessarily represent the official views of the NIH. This work does not represent the views of the Department of Veterans Affairs or the United States Government.

Author contributions

C.-Y.Y., M.S.G., T.A.H., R.A.M. and D.W.L. conceived and designed the experiments. C.-Y.Y., L.C.S.C., J.W.D., G.G.G., M.S.G., I.T.F., M.F.C., A.C.R., C.L.G., R.B., M.M.S., H.H.P. and M.E.T. performed the experiments. C.-Y.Y., M.S.G., T.A.H., G.G.G., R.A.M., J.A.S. and D.W.L. analyzed the data and wrote the manuscript.

Competing interests

D.W.L. has received funding from, and is a scientific advisory board member of, Aeovian Pharmaceuticals, which seeks to develop novel, selective mTOR inhibitors for the treatment of various diseases. The other authors declare no competing interests.

Additional information

Extended data is available for this paper at https://doi.org/10.1038/s43587-024-00744-7.

Supplementary information The online version contains supplementary material available at https://doi.org/10.1038/s43587-024-00744-7.

Correspondence and requests for materials should be addressed to Dudley W. Lamming.

Peer review information *Nature Aging* thanks Stephen Simpson and the other, anonymous reviewers for their contribution to the peer review of this work.

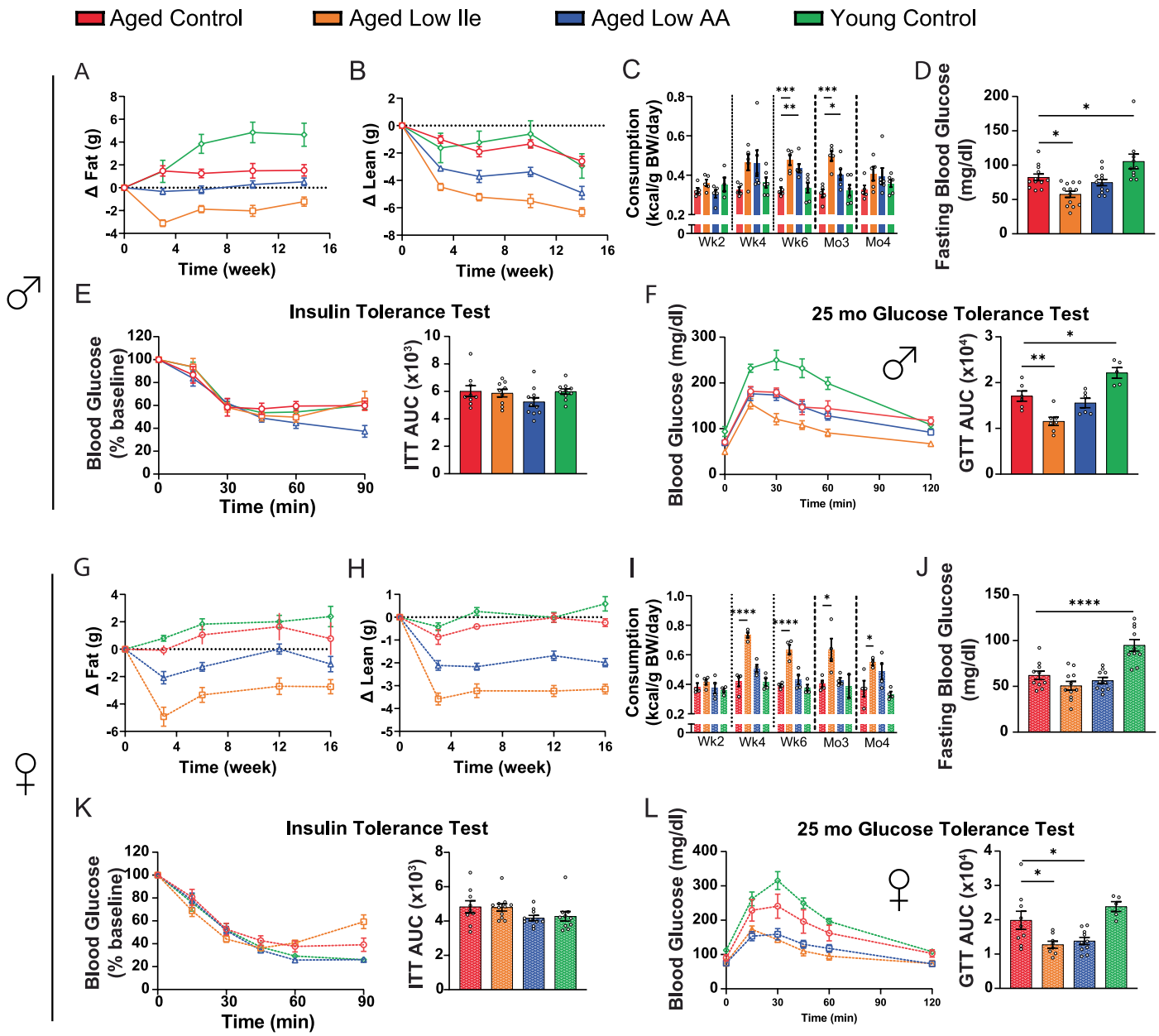
Reprints and permissions information is available at www.nature.com/reprints.

Publisher's note Springer Nature remains neutral with regard to jurisdictional claims in published maps and institutional affiliations.

Springer Nature or its licensor (e.g. a society or other partner) holds exclusive rights to this article under a publishing agreement with the author(s) or other rightsholder(s); author self-archiving of the accepted manuscript version of this article is solely governed by the terms of such publishing agreement and applicable law.

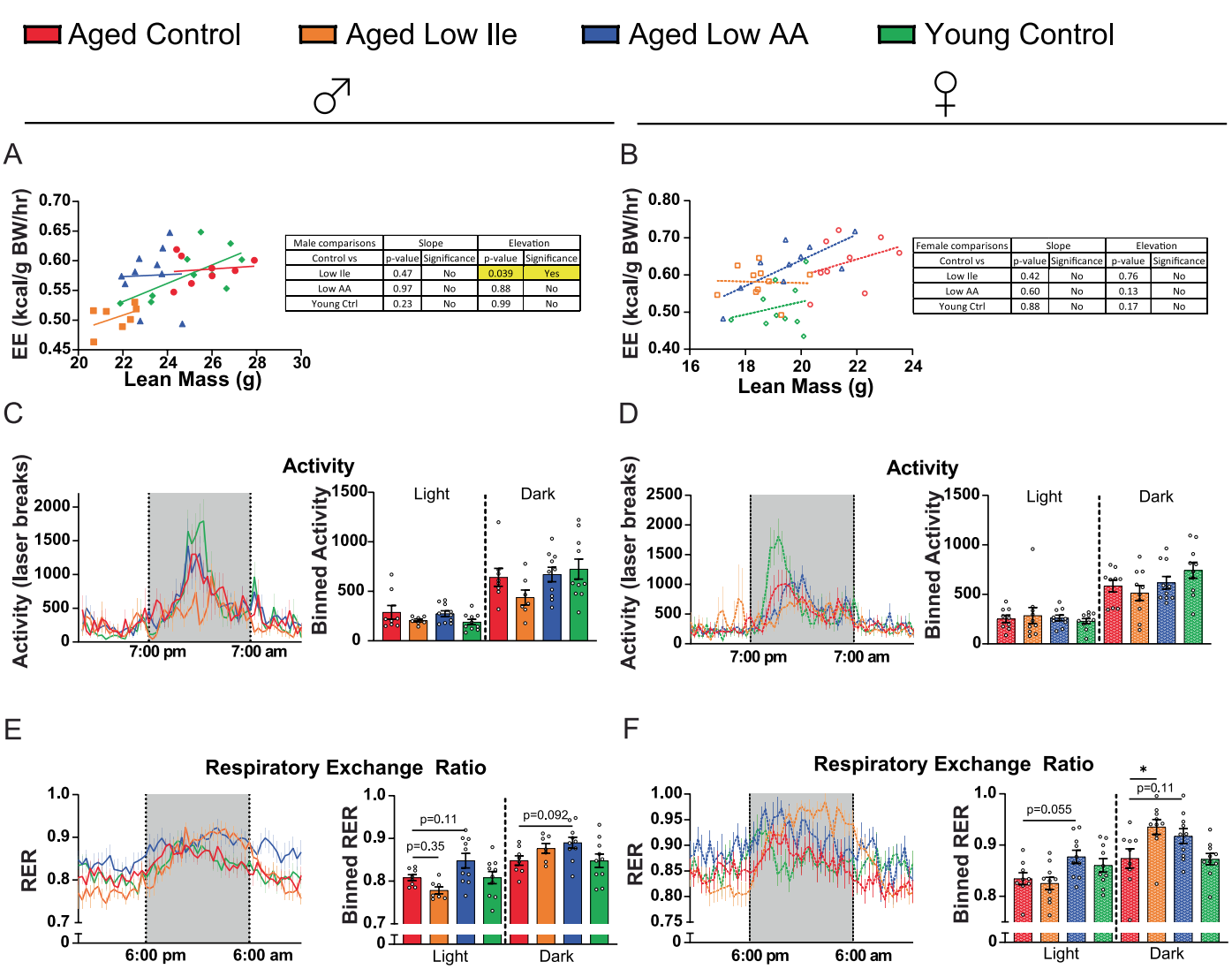
© The Author(s), under exclusive licence to Springer Nature America, Inc. 2024

https://doi.org/10.1038/s43587-024-00744-7



Extended Data Fig. 1 | The effect of late-life feeding of a Low Ile or a Low AA diet on fat and lean mass, food consumption, fasting blood glucose, insulin tolerance, and glucose tolerance at 25 months of age. (A-B) Changes in (**A**) fat and (**B**) lean mass in males over time. (**A-B**) n varies over time, maximum n = 10, 11, 10, and 10. **(C)** Food consumption of male mice throughout the experiment; n varies over time, maximum n = 5, 5, 6, and 6 cages. **(D)** Fasting blood glucose of 21-month-old male after 3 weeks on the indicated diets; n = 12, 13, 12, and 10. **(E)** Insulin tolerance test of 21-month-old male after 4 weeks on the indicated diets; n = 9, 9, 11, and 10. **(F)** Glucose tolerance test in a separate group of 25 months old mice; n = 6, 7, 6, and 5. **(G-H)** Changes in (**G**) fat and (**H**) lean mass in females over time. (G-H) maximum n = 10, 11, 10, and 10. **(I)** Food consumption of female mice throughout the experiment. **(I)** n varies over time, maximum n = 4 cages/group. **(J)** Fasting blood glucose of 21-month-old female mice after 3 weeks on the indicated diets; n = 10, 11, 10, and 10. **(K)** Insulin tolerance test; n = 10, 11, 10, and 10. **(L)** Glucose tolerance test in a separate group of 25 months old mice.; n = 9, 8, 10, and 5. n-value indicate biologically independent animals (or cages if indicated). ANOVA followed by two-sided Dunnett's test vs. Aged Control-fed mice. *p < 0.05, **p < 0.01, ***p < 0.001, ****p < 0.0001. N-values denote biologically independent animals unless otherwise specified and are listed in the order of Aged Control, Aged Low Ile, Aged Low AA, and Young Control. Data presented as mean ± SEM. The exact p-values are provided in Source data.

https://doi.org/10.1038/s43587-024-00744-7

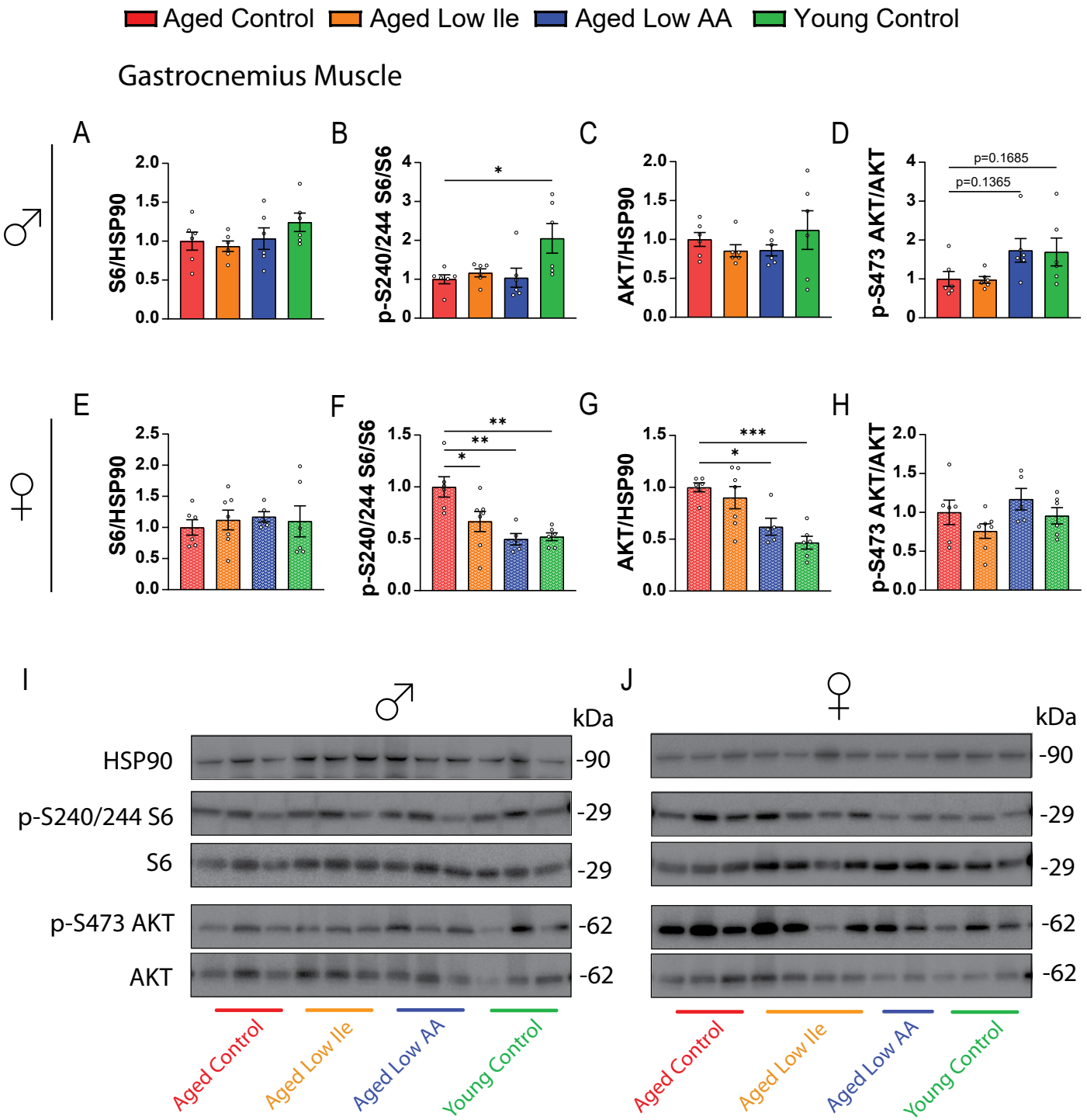


Male comparisons	Slope		Elevation	
Control vs	p-value	Significance	p-value	Significance
Low Ile	0.47	No	0.039	Yes
Low AA	0.97	No	0.88	No
Young Ctrl	0.23	No	0.99	No

Female comparisons	Slope		Elevation	
Control vs	p-value	Significance	p-value	Significance
Low Ile	0.42	No	0.76	No
Low AA	0.60	No	0.13	No
Young Ctrl	0.88	No	0.17	No

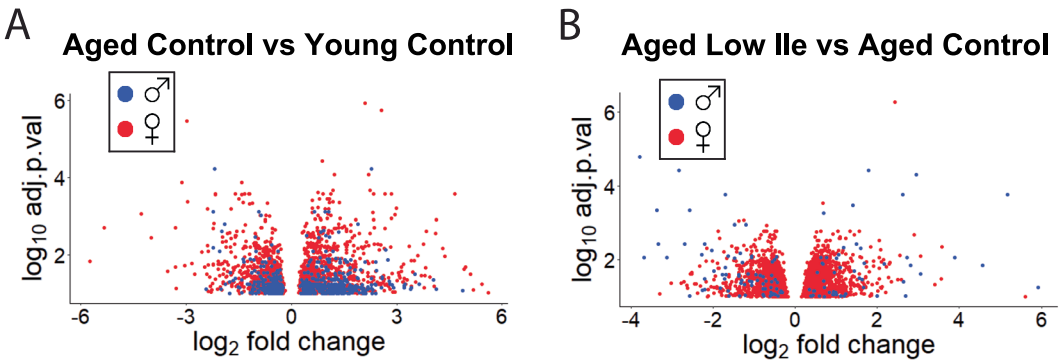
Extended Data Fig. 2 | Effects of late-life Low AA and Low Ile diets on energy balance. (A-B) ANCOVA of energy expenditure with lean mass as a covariate in (**C**) male and (**D**) female mice. **(C-D)** Spontaneous activity of (**E**) male and (**F**) female mice during the metabolic chambers experiments. Shaded period indicates dark phase. **(E-F)** Metabolic chambers were used to determine the respiratory exchange ratio of (**A**) male and (**B**) female mice. Shaded period indicates dark phase. (**A-F**) Male n = 8, 7, 10, and 10; Female n = 9, 10, 10, and 10. N-values denote biologically independent animals unless otherwise specified and are listed in the order of Aged Control, Aged Low Ile, Aged Low AA, and Young Control. *p < 0.05, ANOVA followed by two-sided Dunnett's test; ANOVA conducted separately for the light and dark cycles. Data represented as mean ± SEM. The exact p-values are provided in Source data.

https://doi.org/10.1038/s43587-024-00744-7



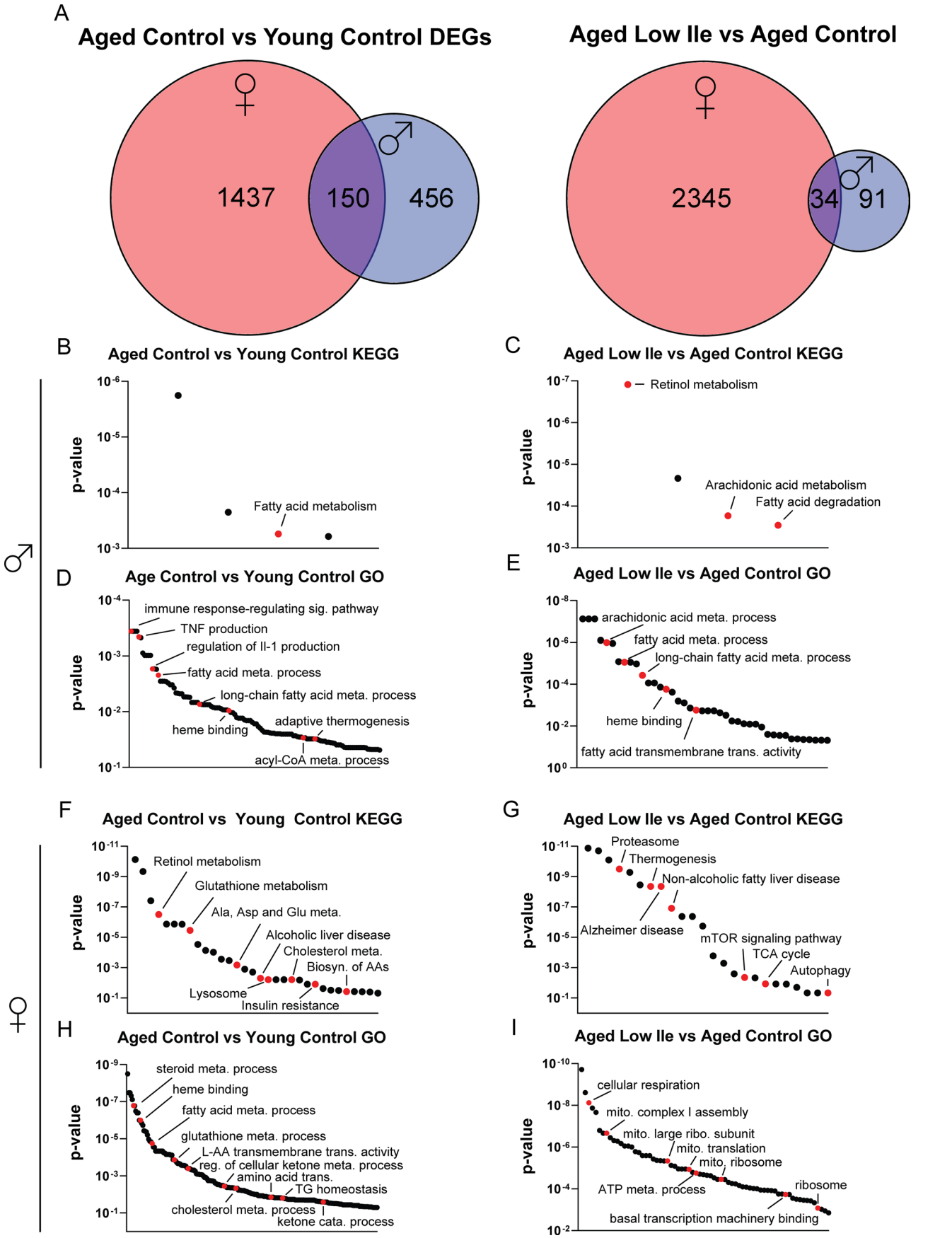
Extended Data Fig. 3 | Western blotting of aging markers in the gastrocnemius muscle. (A-B) Quantification of (**A**) total and (**B**) phosphorylated S6 in male muscle. **(C-D)** Quantification of (**C**) total and (**D**) phosphorylated AKT in male muscle. **(E-F)** Quantification of (**E**) total and (**F**) phosphorylated S6 in female muscle. **(G-H)** Quantification of (**G**) total and (**H**) phosphorylated AKT in female muscle. **(I-J)** Representative Western blots for (**K**) male and (**J**) female mice muscles. For all groups, n = 6. n-value indicates biologically independent animals. *p < 0.05, **p < 0.01, ***p < 0.001 vs. Aged Control mice, ANOVA followed by two-sided Dunnett's test. Data presented as mean ± SEM. The exact p-values are provided in Source data.

https://doi.org/10.1038/s43587-024-00744-7



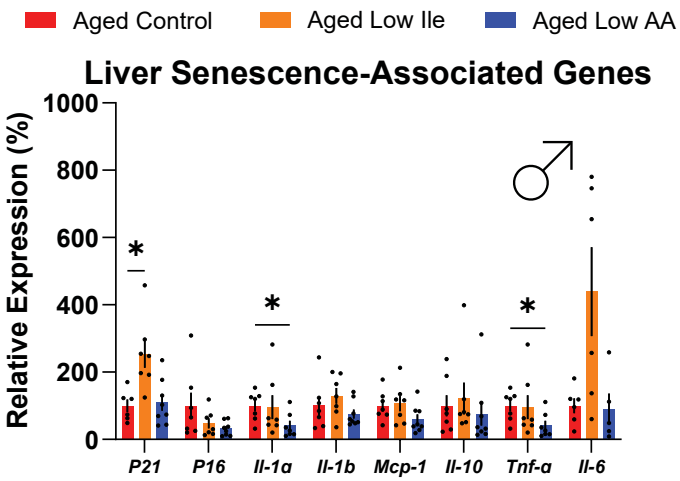
Extended Data Fig. 4 | Volcano plots of hepatic DEGs after Low Ile feeding in aged mice. (A-B) Volcano plots of differentially expressed genes in the liver of (blue) male and (red) female mice with (**A**) age and (**B**) diet. DEGs were identified using an empirical Bayes moderated linear model, and log coefficients and Benjamini-Hochberg (BH) adjusted p-values were generated for each comparison of interest ($\alpha = 0.10$).

https://doi.org/10.1038/s43587-024-00744-7



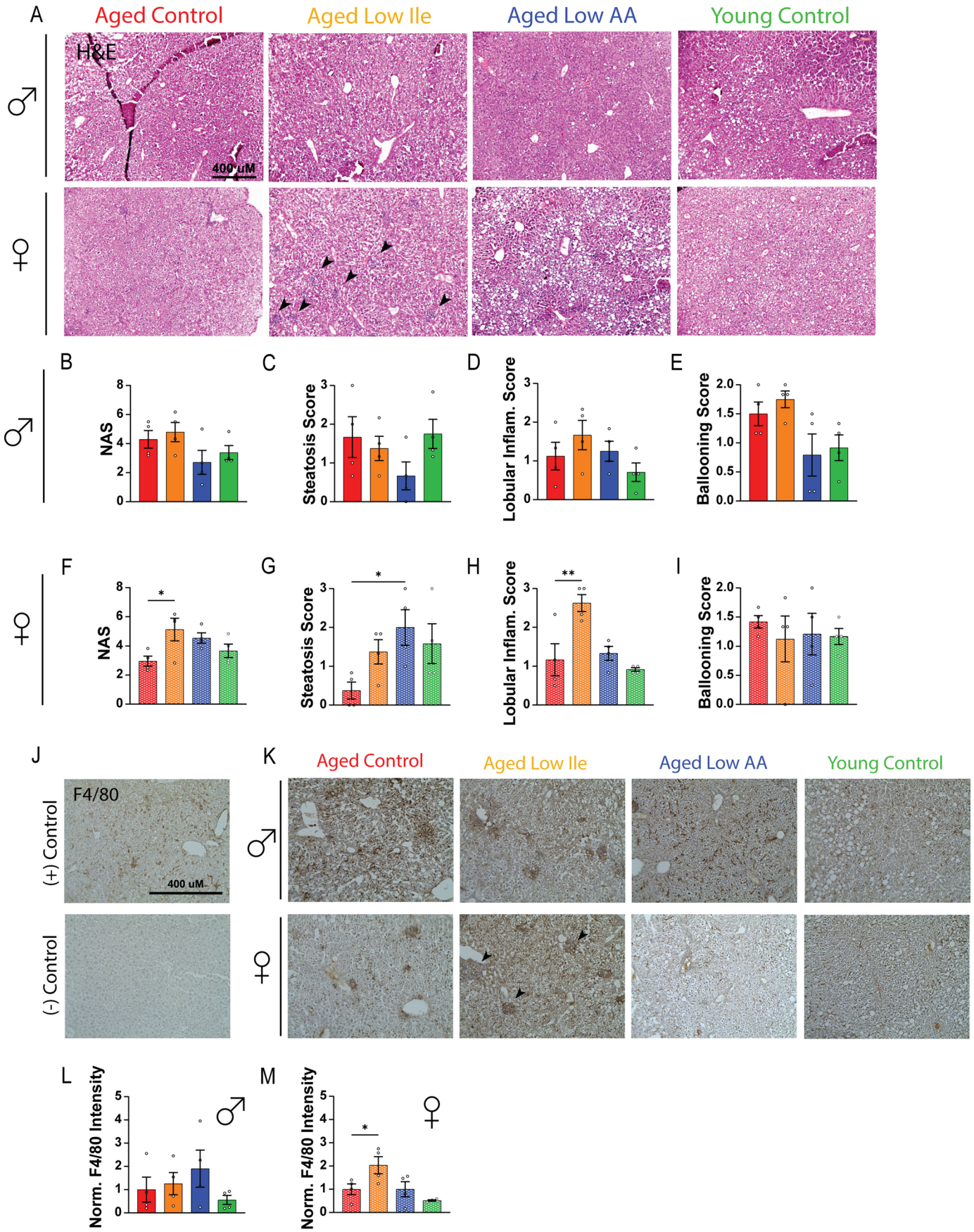
Extended Data Fig. 5 | Venn diagram and enrichment analysis of differentially expressed hepatic genes. **(A)** Venn diagram showing the number of overlapping and non-overlapping (left) age-driven and (right) diet-driven DEGs between male and females. **(B-C)** Significantly enriched KEGG pathways by (**B**) age and (**C**) diet in male mice. **(D-E)** Significantly enriched GO terms by (**D**) age and (**E**) diet in male mice. **(F-G)** Significantly enriched KEGG pathways by (**F**) age and (**G**) diet in female mice. **(H-I)** Significantly enriched GO terms by (**H**) age and (**I**) diet in female mice.

https://doi.org/10.1038/s43587-024-00744-7



Extended Data Fig. 6 | Expression analysis of senescence markers in the aged male liver. Expression of the indicated genes in the livers of 20-month-old mice on the indicated diets for 4 months was determined by qPCR. n = 6 biologically independent animals (*P21* Aged Control, *Il-6* Aged Control, *Il-6* Aged Low Ile), 8 biologically independent animals (*P21* Aged Low AA, *P16* Aged Low AA, *Il1-b* Aged Low AA, *Mcp-1* Aged Low AA, *Il-10* Aged Low AA), 5 biologically independent animals (*Il-6* Aged Low AA), and 7 biologically independent animals for all other groups and genes, *p < 0.05, 2-way mixed-effects analysis (REML) followed by two-sided Dunnett's test vs. Aged Control. Data presented as mean ± SEM. The exact p-values are provided in Source data.

https://doi.org/10.1038/s43587-024-00744-7

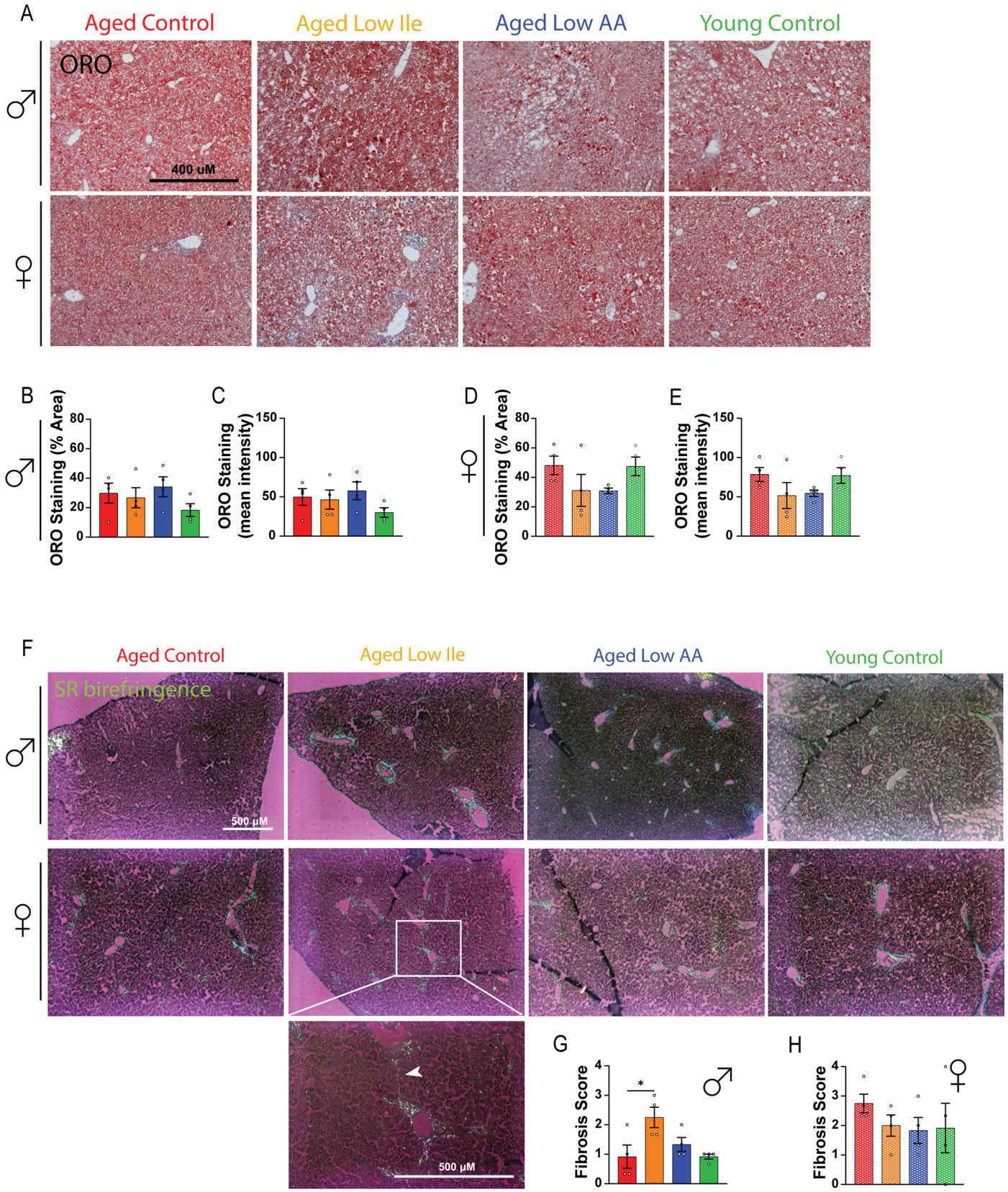


Extended Data Fig. 7 | See next page for caption.

https://doi.org/10.1038/s43587-024-00744-7

Extended Data Fig. 7 | H&E and F4/80 staining of the mice liver. **(A)** Representative hematoxylin and eosin (H&E) staining of the mouse liver. Black arrows mark extramedullary hematopoiesis, indicative of lobular inflammation. **(B-I)** Quantification of (**B**-**E**) male and (**F**-**I**) female H&E staining in Nonalcoholic Fatty Liver Disease Activity Score (NAS) score and its component scores: steatosis, lobular inflammation, and hepatocyte ballooning. **(J)** Positive and negative control (without antibody) staining of the mouse liver with the F4/80 antibody. **(K)** Representative F4/80 staining of the mouse liver. Black arrows mark loci of extramedullary hematopoiesis, indicative of lobular inflammation, similar to the H&E staining. **(L-M)** Quantification of (**L**) male and (**M**) female F4/80 staining mean intensity. For all groups n = 4. *$p < 0.05$, **$p < 0.01$, ANOVA followed by two-sided Dunnett's test vs. Aged Control. Data presented as mean ± SEM. A blinded evaluator scored the sections three times and the average score for each animal was taken for statistical analysis. The exact p-values are provided in Source data.

https://doi.org/10.1038/s43587-024-00744-7



Extended Data Fig. 8 | Oil Red O and Sirius Red staining of the mice liver. (A) Representative oil red O (ORO) staining of the mouse liver. **(B-E)** Quantification of (**B-C**) male and (**D-E**) female ORO staining in % area and mean intensity. **(F)** Representative polarized light microscopy of the Sirius Red (SR) staining birefringence in the mouse liver. White arrow highlights bridging, an indication of advanced liver fibrosis. **(G-H)** Quantification of male (**G**) and female (**H**) liver fibrosis score. For all groups n = 4. ANOVA followed by two-sided Dunnett's test vs. Aged Control. *p < 0.05. Data presented as mean ± SEM. A blinded evaluator scored the sections three times and the average score for each animal was taken for statistical analysis. The exact p-values are provided in Source data.

https://doi.org/10.1038/s43587-024-00744-7

Extended Data Table 1 | The composition and calorie content of the diets used in this study

Diet	Control	Low Ile	Low AA
Teklad ID	TD.140711	TD.160734	TD.140712
Kcal/g	3.9	3.9	3.9
kcal protein	22.0%	22.0%	**7.1%**
kcal CHO	59.4%	59.4%	**74.4%**
kcal fat	18.6%	18.6%	18.5%
Amino acids g/kg			
L-Alanine	9.38	9.83	**3.05**
L-Arginine	6.30	6.30	**2.05**
L-Asparagine	20.58	20.91	**6.70**
L-Aspartic Acid	20.58	21.25	**6.70**
L-Cystine	7.20	7.20	**2.34**
L-Glutamic Acid	28.97	29.71	**9.43**
L-Glutamine	33.77	34.14	**11.00**
Glycine	2.96	3.34	**0.96**
L-Histindine HCl, monohydrate	4.60	4.60	**1.50**
L-Isoleucine	7.80	**2.54**	**2.54**
L-Leucine	25.40	25.40	**8.27**
L-Lysine HCl	20.38	20.38	**6.64**
L-Methionine	6.70	6.70	**2.18**
L-Phenylalanine	6.60	6.60	**2.15**
L-Proline	7.41	7.99	**2.41**
L-Serine	7.41	7.94	**2.41**
L-Threonine	9.70	9.70	**3.16**
L-Tryptophan	3.40	3.40	**1.10**
L-Tyrosine	6.90	6.90	**2.25**
L-Valine	8.40	8.40	**2.74**
Sucrose	291.25	291.25	291.25
Corn Starch	150.00	150.61	232.43
Maltodextrin	150.00	150.61	232.43
Corn Oil	52.00	52.00	52.00
Olive Oil	29.00	29.00	29.00
Cellulose	30.00	30.00	30.00
Mineral Mix, AIN-93M-MX (94049)	35.00	35.00	35.00
Calcium Phosphate, monobasic, monohydrate	8.20	8.20	8.20
Vitamin Mix, Teklad (40060)	10.00	10.00	10.00
BHQ, antioxidant	0.012	0.012	0.012
Food color (0.1 g/kg)	Red	Orange	Blue

Bolded terms highlights the intended manipulations in each diet.

https://doi.org/10.1038/s43587-024-00744-7

Extended Data Table 2 | Complete Echocardiogram Dataset

Male	Aged Control		Aged Low Ile		Aged Low AA		Young Control		
	Mean	SEM	Mean	SEM	Mean	SEM	Mean	SEM	Sig. vs Aged Control
Weight (g)	31.57	1.38	25.86	1.22	29.40	0.81	29.20	0.80	Aged Low Ile (n=6,7,5,5; p=0.0042)
LV Mass (AW) (mg)	109.33	6.74	121.50	12.18	105.32	7.15	90.72	2.86	
LV Mass/BW (mg)	3.49	0.25	4.76	0.51	3.58	0.18	3.11	0.07	Aged Low Ile (n=6,7,5,5; p=0.0382)
LVID;d (mm)	4.45	0.11	4.61	0.13	4.46	0.14	4.17	0.08	
LVPW;d (mm)	0.65	0.03	0.69	0.03	0.63	0.02	0.61	0.03	
LVID;s (mm)	3.48	0.15	3.69	0.17	3.47	0.11	3.31	0.06	
LVPW;s (mm)	0.80	0.04	0.81	0.03	0.78	0.02	0.74	0.03	
LVAW;d (mm)	0.66	0.02	0.66	0.03	0.64	0.03	0.64	0.02	
LVAW;s (mm)	0.80	0.04	0.81	0.03	0.82	0.01	0.75	0.02	
LV Vol;d (μL)	90.70	5.44	98.46	6.68	91.19	7.11	77.69	3.61	
LV Vol;s (μL)	50.84	5.05	59.13	6.64	50.20	4.20	44.57	1.82	
EF (%)	44.54	2.66	40.84	3.26	44.90	1.75	42.56	0.72	
FS (%)	22.04	1.54	20.04	1.83	22.18	1.03	20.68	0.43	
IVRT (ms)	19.12	1.47	17.27	1.68	20.11	1.82	17.28	1.11	
Stroke Volume (μL)	39.86	1.52	39.34	2.31	40.99	3.47	33.12	1.91	
Heart Rate (bpm)	489.49	21.43	476.81	21.14	517.75	26.71	480.92	24.60	
Cardiac Output (mL/min)	20.37	1.21	19.11	1.10	19.67	1.96	16.71	1.35	
Ao Area (cm)	1.49	0.20	2.24	0.38	1.25	0.18	1.06	0.07	
Ao Mean Vel (mm/s)	717.31	74.51	512.96	34.50	818.39	91.26	734.91	21.09	Aged Low Ile (n=6,6,4,5; p=0.0473)
Ao Mean Grad (mmHg)	2.17	0.47	1.08	0.14	2.78	0.60	2.17	0.13	
Ao Peak Vel (mm/s)	1277.76	112.74	892.86	64.41	1434.55	168.96	1287.00	36.04	Aged Low Ile (n=6,6,4,5; p=0.0245)
Ao Peak Grad (mmHg)	6.79	1.24	3.27	0.47	8.58	1.98	6.65	0.38	
Ejection Time (ms)	44.12	3.15	38.47	2.68	40.35	2.63	43.69	1.87	

Female	Aged Control		Aged Low Ile		Aged Low AA		Young Control		
	Mean	SEM	Mean	SEM	Mean	SEM	Mean	SEM	Sig. vs Aged Control
Weight (g)	28.63	1.73	23.13	0.48	28.20	0.85	24.00	1.52	Aged Low Ile (n=8,8,10,5; p=0.0068)
LV Mass (AW) (mg)	103.13	9.38	79.45	9.35	96.27	4.32	71.29	5.47	Young Control (n=8,8,10,5; p=0.0363)
LV Mass/BW (mg)	3.73	0.45	3.47	0.45	3.43	0.16	2.98	0.17	
LVID;d (mm)	4.42	0.09	3.92	0.19	4.39	0.11	4.11	0.11	Aged Low Ile (n=8,8,10,5; p=0.0374)
LVPW;d (mm)	0.62	0.04	0.60	0.02	0.58	0.02	0.50	0.02	Young Control (n=8,8,10,5; p=0.0395)
LVID;s (mm)	3.47	0.08	3.08	0.21	3.45	0.10	3.31	0.17	
LVPW;s (mm)	0.76	0.04	0.72	0.02	0.72	0.01	0.61	0.01	Young Control (n=8,8,10,5; p=0.0019)
LVAW;d (mm)	0.64	0.03	0.60	0.02	0.63	0.02	0.54	0.02	Young Control (n=8,8,10,5; p=0.0235)
LVAW;s (mm)	0.79	0.03	0.73	0.01	0.74	0.01	0.69	0.03	Young Control (n=8,8,10,5; p=0.0271)
LV Vol;d (μL)	88.96	4.07	68.42	8.30	87.88	5.10	75.21	5.05	
LV Vol;s (μL)	50.07	2.80	39.32	7.00	49.91	3.38	45.20	5.77	
EF (%)	43.88	1.05	44.68	3.34	43.44	1.56	40.68	3.87	
FS (%)	21.59	0.59	21.97	1.90	21.34	0.86	19.73	2.12	
IVRT (ms)	20.72	2.32	16.63	1.72	20.50	1.60	19.33	1.88	
Stroke Volume (μL)	38.90	1.64	29.10	2.00	37.97	2.40	30.01	1.83	Aged Low Ile (n=8,8,10,5; p=0.0078), Young Control (p=0.0385)
Heart Rate (bpm)	417.71	24.83	535.23	22.28	496.71	19.80	480.11	26.98	Aged Low Ile (n=8,8,10,5; p=0.0031), Aged Low AA (p=0.0409)
Cardiac Output (mL/min)	18.77	1.28	15.37	1.16	18.67	1.14	14.29	1.45	
Ao Area (cm)	1.08	0.11	1.00	0.06	1.30	0.11	1.10	0.08	
Ao Mean Vel (mm/s)	783.91	78.03	682.80	30.99	714.48	51.60	650.10	42.24	
Ao Mean Grad (mmHg)	2.63	0.57	1.91	0.17	2.14	0.28	1.72	0.22	
Ao Peak Vel (mm/s)	1405.10	137.05	1189.40	53.96	1256.36	102.35	1126.18	77.47	
Ao Peak Grad (mmHg)	8.43	1.76	5.78	0.51	6.70	0.95	5.17	0.72	
Ejection Time (ms)	48.47	2.56	42.01	1.60	42.64	1.56	42.11	2.17	

Detailed male and female echocardiogram dataset in mice after 6 weeks of dietary intervention starting from 24 months of age. N-values are listed in the order of Aged Control, Aged Low Ile, Aged Low AA, and Young Control. 1-way ANOVA with two-sided Dunnett's post-test.

nature portfolio

Corresponding author(s): Dudley Lamming

Last updated by author(s): Sep 16, 2024

Reporting Summary

Nature Portfolio wishes to improve the reproducibility of the work that we publish. This form provides structure for consistency and transparency in reporting. For further information on Nature Portfolio policies, see our Editorial Policies and the Editorial Policy Checklist.

Statistics

For all statistical analyses, confirm that the following items are present in the figure legend, table legend, main text, or Methods section.

n/a	Confirmed
☐	☒ The exact sample size (*n*) for each experimental group/condition, given as a discrete number and unit of measurement
☐	☒ A statement on whether measurements were taken from distinct samples or whether the same sample was measured repeatedly
☐	☒ The statistical test(s) used AND whether they are one- or two-sided *Only common tests should be described solely by name; describe more complex techniques in the Methods section.*
☐	☒ A description of all covariates tested
☐	☒ A description of any assumptions or corrections, such as tests of normality and adjustment for multiple comparisons
☒	☐ A full description of the statistical parameters including central tendency (e.g. means) or other basic estimates (e.g. regression coefficient) AND variation (e.g. standard deviation) or associated estimates of uncertainty (e.g. confidence intervals)
☐	☒ For null hypothesis testing, the test statistic (e.g. *F*, *t*, *r*) with confidence intervals, effect sizes, degrees of freedom and *P* value noted *Give P values as exact values whenever suitable.*
☒	☐ For Bayesian analysis, information on the choice of priors and Markov chain Monte Carlo settings
☒	☐ For hierarchical and complex designs, identification of the appropriate level for tests and full reporting of outcomes
☒	☐ Estimates of effect sizes (e.g. Cohen's *d*, Pearson's *r*), indicating how they were calculated

Our web collection on statistics for biologists contains articles on many of the points above.

Software and code

Policy information about availability of computer code

Data collection	Software used to capture the data includes metabolic chambers (Oxymax v5.64), body composition (EchoMRI v140320), and camera tracking (Ethovision XT v15.0.14.16).
Data analysis	Data in this paper was analyzed using R (v4.2.2) and GraphPad Prism (v9).

For manuscripts utilizing custom algorithms or software that are central to the research but not yet described in published literature, software must be made available to editors and reviewers. We strongly encourage code deposition in a community repository (e.g. GitHub). See the Nature Portfolio guidelines for submitting code & software for further information.

Data

Policy information about availability of data

All manuscripts must include a data availability statement. This statement should provide the following information, where applicable:

- Accession codes, unique identifiers, or web links for publicly available datasets
- A description of any restrictions on data availability
- For clinical datasets or third party data, please ensure that the statement adheres to our policy

RNA-seq data has been deposited with the Gene Expression Omnibus, accession number GSE254721. The raw heart lipidomics data has been deposited with MassIVE, identifier MSV000095324. The data that support the plots within this article and other findings of this study, including full scans of western blot images, are provided as Source Data files.

Research involving human participants, their data, or biological material

Policy information about studies with human participants or human data. See also policy information about sex, gender (identity/presentation), and sexual orientation and race, ethnicity and racism.

Reporting on sex and gender	N/A
Reporting on race, ethnicity, or other socially relevant groupings	N/A
Population characteristics	N/A
Recruitment	N/A
Ethics oversight	N/A

Note that full information on the approval of the study protocol must also be provided in the manuscript.

Field-specific reporting

Please select the one below that is the best fit for your research. If you are not sure, read the appropriate sections before making your selection.

☒ Life sciences ☐ Behavioural & social sciences ☐ Ecological, evolutionary & environmental sciences

For a reference copy of the document with all sections, see nature.com/documents/nr-reporting-summary-flat.pdf

Life sciences study design

All studies must disclose on these points even when the disclosure is negative.

Sample size	Sample size was determined based on our previous experimental results with the effects of Low Isoleucine diet feeding, as published in Yu and Richardson et al., 2021, Cell Metabolism. For in vivo experiments, we utilized power calculation (>90% power to detect a change in area under the curve during a glucose tolerance test, $p < 0.05$) as based on the results of our previous published research.
Data exclusions	In the transcriptomic analysis of the liver, one Low Ile-fed female was excluded as it was a significant outlier from all groups following PCA analysis.
Replication	The assays were chosen based on the evaluation of a number of criteria including good reproducibility, and are widely utilized by multiple groups. The Low Ile and Low AA diets successfully reproduced results found in our previous studies in younger male mice. All data derived from animal experiments represent the results obtained from at least five biological independent animals. As these were studies using aged mice, there was no attempts at replication, but animals were assessed for multiple phenotypes at multiple time points and these assessments are included in the manuscript.
Randomization	Aged mice obtained from the NIA were randomized into groups of equivalent weight, body composition, and frailty to the best of our ability prior to commencement of the study, with 2-3 mice housed per cage where possible.
Blinding	Investigators were blinded to diet groups during data collection whenever feasible, but this was not usually possible or feasible as cages were clearly marked to indicate the diet provided, diets were color-coded to prevent feeding mistakes, and the size and body composition of the mice was altered by the diet. Researchers are blinded to group allocations during image analysis. During analysis of other dataset, the investigators are not blinded as the results are objective quantifications.

Reporting for specific materials, systems and methods

We require information from authors about some types of materials, experimental systems and methods used in many studies. Here, indicate whether each material, system or method listed is relevant to your study. If you are not sure if a list item applies to your research, read the appropriate section before selecting a response.

Materials & experimental systems

n/a	Involved in the study
☐	☒ Antibodies
☒	☐ Eukaryotic cell lines
☒	☐ Palaeontology and archaeology
☐	☒ Animals and other organisms
☒	☐ Clinical data
☒	☐ Dual use research of concern
☒	☐ Plants

Methods

n/a	Involved in the study
☒	☐ ChIP-seq
☒	☐ Flow cytometry
☒	☐ MRI-based neuroimaging

Antibodies

Antibodies used

Cell Signaling Technology: ULK1 (8054), pULK-S757 (14202), S6K1 (2708), pS6K1-T389 (9234), S6 (2217), pS6-S240/244 (2215), pS6-S235/236 (2211), eif2α (5324), peif2a-S51 (3597), 4E-BP1 (9644), and p4E-BP1-T37/46 (2855), AKT (9272), pAKT-T308 (2965), MK2 (12155), ACACA1 (4190) pAKT-S473 (9271), NDRG1 (9408), pNDRG1-T346 (5482), eIF4E (9742), peIF4E-S209 (9741), HSP70 (4872), MEK1 (12671), pMEK1-S217 (9154), ERK 1-2 (4695), pERK 1-2-T202 (9101), MNK1 (2195). Bioss: MNK2 (17697). Origene: TFAM (720347). Invitrogen: pMNK (700242), pMNK-T197 (700242). Abcam: FASN (22759), ACLY (40793). ABclonal: PLIN1 (A4758). ThermoFisher: PLIN3 (PA1-46161). Bio-Rad: F4/80 (MCA497G).

Validation

All antibodies were validated for use in mice by the manufacturer and validation descriptions are available on their respective websites. Specificity of antibodies has also been validated by the authors in previous publications, including Richardson et al. 2021, Nature Aging, Jiang et al. 2023 Life Sci, Shen et al. 2021, Aging Cell. F4/80 antibody is validated using positive and negative staining control.

Animals and other research organisms

Policy information about studies involving animals; ARRIVE guidelines recommended for reporting animal research, and Sex and Gender in Research

Laboratory animals

C57BL/6J.NIA male and female mice at 6 months of age, 20 months of age, and 22 months of age were used.

Wild animals

No wild animals were used in the study.

Reporting on sex

As sex differences in the response to diets were major findings in this manuscript, whether an effect applies to one sex or both is clearly indicated and the resulting statistical analysis are done separately.

Field-collected samples

No field-collected samples were used in the study.

Ethics oversight

Animal studies were approved by the Institutional Animal Care and Use Committee of the William S. Middleton Memorial Veterans Hospital, Madison, WI.

Note that full information on the approval of the study protocol must also be provided in the manuscript.

Plants

Seed stocks

N/A

Novel plant genotypes

N/A

Authentication

N/A